2013년 2월
석사학위 논문

실버나노입자의 열처리분위 기가 입자모양에 미치는 영향

조선대학교 대학원

첨단부품소재공학과(소재공학전공)

만달 칸칸프로사드

실버나노입자의 열처리분위 기가 입자모양에 미치는 영향

Effect of surface faceting and heat-treatment atmosphere on particle shape of silver nanoparticle

2013년 2월 25일

조선대학교 대학원

첨단부품소재공학과(소재공학전공)

만달 칸칸프로사드

실버나노입자의 열처리분위 기가입자모양에 미치는 영향

지도교수 신 동 찬

이 논문을 공학 석사학위신청 논문으로 제출함

2012년 110월

조선대학교 대학원

첨단부품소재공학과(소재공학전공)

만달 칸칸프로사드

만달 칸칸프로사드의 석사학위 논문을 인준함

위원장 조선대학교 교 수 이종국 (인)

위 원 조선대학교 교 수 강현철 (인)

위 원 조선대학교 부교수 신동찬 (인)

2012년 11 월

조선대학교 대학원

Content

List of Table

List of Figures

초 록

실버나노입자의 열처리분위기가입자모양에 미치는 영향

만달칸칸프로사드
지도교수 : 신동찬
천단부품소재공학과(소재전공)
조선대학교 대학원

본 연구에서는 스핀 코팅법을 통하여 실버박막 제조하고 열처리온도와 열처리분위기가 입자 모양에 미치는 영향에 대하여 조사하였다. 실버나노 페이스트 점성은 실버량이 74 wt% 함유된 실버페이스트 중에 에탄올을 첨가하여 점성을 조절하였다. 스핀코팅법에 통하여 실버 코팅막을 제조하기 위하여 스핀 속도를 1000에서 5000 rpm으로 조절하였으며 코팅시간은 30초로 하였다. 스핀코팅된 실버박막은 열처리온도 60°C 에서 600°C 사이에서 1시간동한 열처리한 후 4 포인트 프로브를 통하여 면저항을 측정하였다. 저온에서 열처리한 시편에서는 분위기에 따라 구형, 각진형태 울퉁불퉁한 형태로 비등방성을 갖는 입자모양을 나타내었으며 고온에서는 등방성을 형태의 입자모양을 나타내었다. 실버전극은 OLED 조명, 디스플레이, PDP 디스플레이에 사용되고 있다.

ABSTRACT

Effect of surface faceting and heat-treatment atmosphere on particle shape of silver nanoparticle

Mandal Kankan Prosad
Advisor : Dong Chan Shin, Ph.D.
Department of Advanced Parts and Materials Engineering
Graduate School of Chosun University

When spin coated silver nanolayer was annealed in different atmosphere and temperature at high temperature nano particle became atomically rough surface, spherical, defaceted and isotropic energy surface but at low temperature nanoparticle became polygonal, atomically smooth surface, singular and nonisotropic energy surface. The singular surface facilitated to form faceted surface. The faceted surface facilitated to form bimodal growth where as defaceted surface facilitated to form normal grain growth. Silver nano powder showed lower faceting to defaceting transition temperature compare to polycrystalline silver. The experimental results showed that normal grain growth predominated above the critical transition temperature due to defaceted rough surface eliminates some cups at high temperature. We have annealed silver nanoparticle after spin coating form 60^{o}C to 600^{o}C. And conductivity was measured by 4 point probe. Silver electrode is used in OLED display, Plasma display and OLED lighting device.

1. Introduction

Theoretically, Crystal with high surface tension will not liberate more energy during growth of its interface then the interface will not be temporary heated. The growth rate will be slow. That will result 2D growth of interface. In other words then faceted interface will be formed. At low temperature all crystal are equilibrium with surrounding fluid are predicted [1,2,3] and have been observed to have atomically flat (or smooth or singular) surfaces of low index planes hence polyhedral shapes. Following the proposal[4] the roughening transition of the crystal surface has been extensively studied both theoretically [5] and experimentally using the diffraction techniques [6] and indirectly by observing the macroscopic shape changes [7]. The growth of crystals with either smooth or rough surface has also been studied extensively, and it has now been fairly well established that the smooth surfaces grow by two-dimensional nucleation of steps if they do not have defects. The growth of rough surfaces is controlled by diffusion in the surrounding fluid and often becomes dendritic.

For system of grains dispersed in multicomponent liquid matrix, abnormal grain coarsening occurs only if the grains have polyhedral shapes and normal coarsening if they are spherical. In certain materials such as NbC-Co,[8,9] the surface roughening transition occurs at high temperatures with concurrent changes of the grain shape and the growth behaviour. The abnormal coarsening of the polyhedral grains occurred by two-dimensional nucleation of surface steps or by spiral growth on surface defects[10]. The spherical grains with a rough surface grow normally with the rate determined by diffusion in the liquid matrix.

Recently, it has been proposed that the same correlation exists in single-phase polycrystals between the grain boundary structure and the grain coarsening behaviour, as indicated by the observations in Ni.[11,12]. There have possibility of the roughening transition of low-angle grain boundaries[13] and Various indirect experimental evidence have been done to determine roughening transition temperature of grain boundaries in pure metals, which were observe to occur in the temperature ranges between about 0.3 and 0.9 T_m, where T_m is the melting point[14]. The coincidence site lattice (CSL) type boundaries in Al and Au [15] and even the general boundaries in Ni[16] were observed to be faceted

at low temperature and undergo defaceting transitions at temperatures above $0.5T_m$. Oxygen in Ni,[17] Cu,[18] and Fe[19] were found to induce faceting of grain boundaries. If grain boundaries are faceted, it is likely that at least some of the facet planes have singular structures corresponding to the cusps in the plot of the grain boundary energy γ against the inclination angle or the normal direction. The defaceting transition occurs when the average grain boundary normal corresponds to a curved segment of the equilibrium shape (of a grain embedded in another) or a convex segment of the reciprocal γ plot [20,21]. When a faceted grain boundary undergoes the defaceting transition, it becomes smoothly curved macroscopically and should have a rough atomic structure.[22]

In Ni it was observed [23] that abnormal grain growth (AGG) occurred when the grain boundaries were faceted at low temperatures and normal growth when they were defaceted at high temperatures. It was proposed [24] that AGG occurred if the faceted grain boundaries migrated either by two-dimensional nucleation of the boundary steps or by spiral growth on defects. Such mechanisms for the grain boundary migration have been suggested [25,26,27] based on the observations of spiral growth of grain boundaries and formation of annealing twins.

The purpose of this work is to test the correlation between the grain coarsening behaviour, either abnormal or normal, and grain boundary shape, either faceted or defaceted in Ag. It is found that the faceting of the surface and grain boundaries were similarly dependent on the atmosphere. Therefore the atmosphere for the heat-treatment was also varied from oxygen to nitrogen because of the possible effect on grain boundary faceting and hence AGG behaviour. Oxygen atmosphere will increase work function of silver hence it can be used as hole supplying electrode for OLED. It can do so by increasing facet formation. The macroscopic view of grain boundary is also related to formation of super lattice (Coincidence site lattice) at grain boundary.

II. Research background

A. Motivation

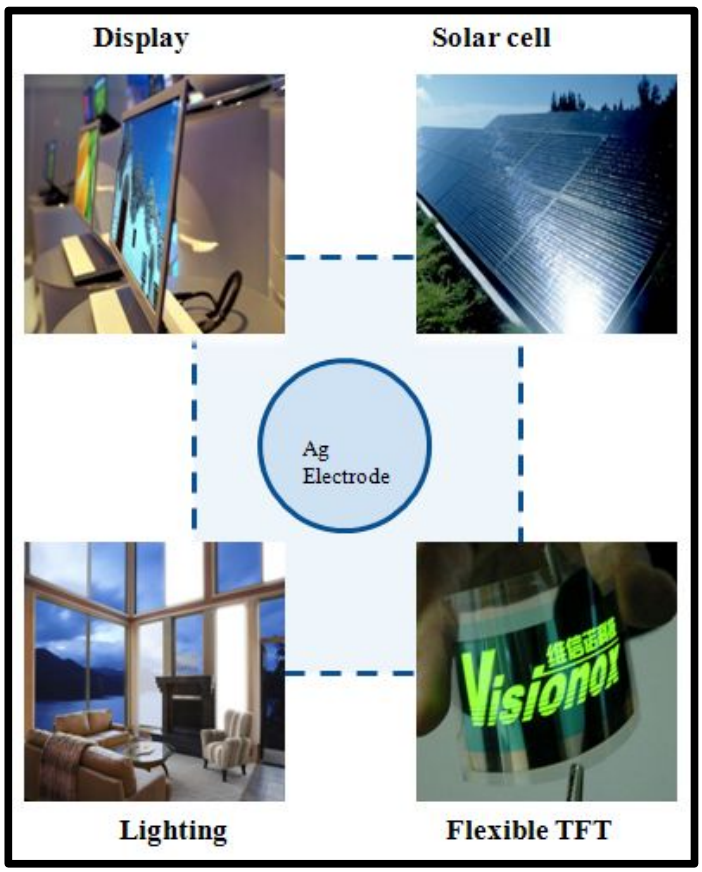

Fig. 1. Application of Ag electrode.

Silver (Ag) has versatile application among these in PDP (plasma display panel) electrodes, RFID (radio frequency identification), FPCB (flexible printed circuit board), EMI (electro magnetic interference), solar cell (OSC) and display (OLED) can be highlighted. Fig.1 Shows some application of silver electrode on solar cell, display, lighting and flexible TFT devices.

Fig. 2(a) shows the position of typical Ag electrode in OLED lighting and Fig. 2(b), 2(c),2(d),2(e),2(f),2(g),2(h) shows the typical example of probable structure of Ag material on glass. Fig. 2(b) shows that silver form single crystal on glass. Fig. 2(c) shows that large grains of Ag are distributed on glass. Fig. 2(d) shows that big Ag grains are distributed in small silver grains on glass and that are connected with each other. Fig. 2(e) shows that big Ag particles are distributed uniformly and all are connected. Fig. 2(f) shows that small Ag particles are distributed on glass and all are connected. Fig. 2(g) shows that big Ag particles are distributed in small silver particles and that are connected. Fig. 2(h) shows that all silver particles are separated. This is the worst case because in this case conductivity is lowest. Among this fig 2(d,g,h) are textured and if faceted structure produced then fine scale textured structure, we can expect.

I have produced Fig. 2(c), 2(d) and 2(h) types Ag structure. SEM images of that will be shown in result and discussion section.

B. Properties of Nanoparticle

Nanoparticle has excessively high surface area to volume ratio compare to micro size particle. Crystallographically the lattice prameter for nanoparticle will be high compare to microparticle. That's why nanoparticle structure should be quasi-crystaline structure. For single component nanoparticle , no charge imbalance will be observed on surface of nanoparticle except weak van der waals force but for multi component nanoparticle according to crystallographic consideration tremendous surface charge will be created on surface of nanoparticle. Here compare to volume developed zeta potential will be high .

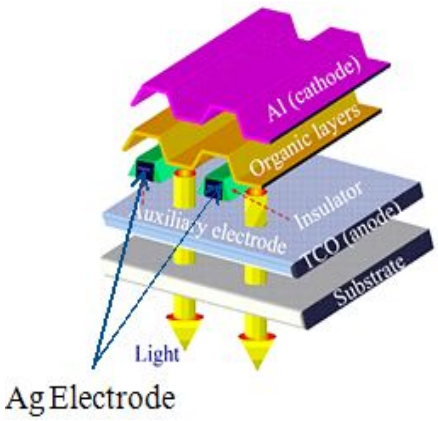

(a) OLED lighting device

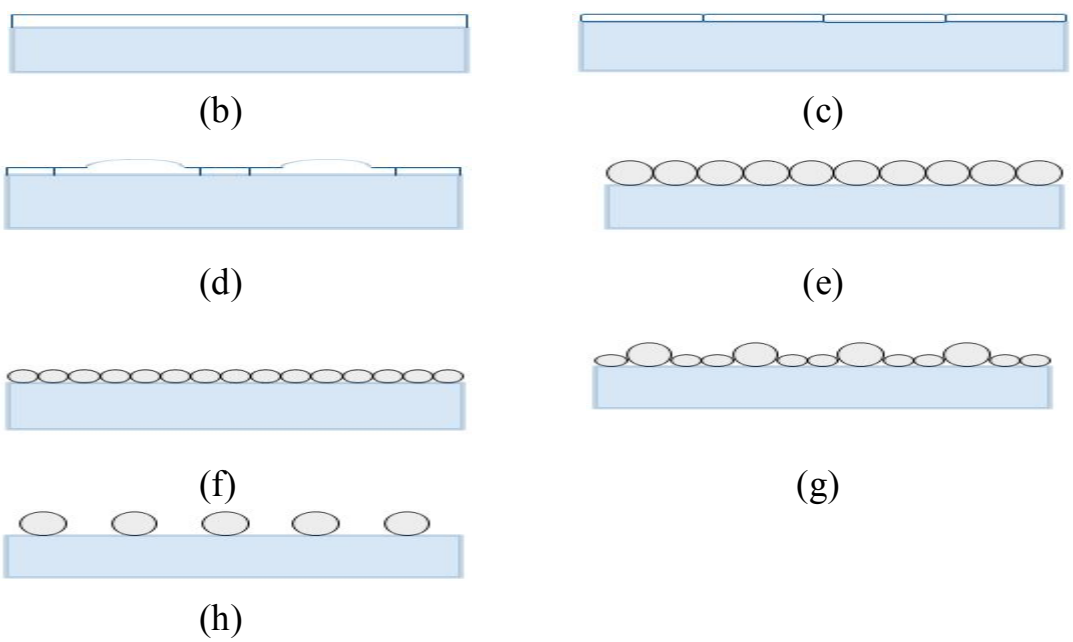

Fig. 2. Example of Ag Electrode in OLED Lighting (a) and probable Ag Electrode Structure. (b, c, d, e, f, g, h).

During making of solution with nanoparticle due to avoid agglomeration some polymer material is generally used to avoid agglomeration. Once this polymer chain form on naoparticle then it will help to avoid agglomeration by changing zeta potential on surface of particle.

Because nanoparticle is small, driving force of sintering of nanoparticle is very high and grain boundary will be moved very easily. Also grain boundary potential will be low for after sintered nanoparticle. For very thin film at low temperature faceted grain will be formed. The grain boundary then will be connected at top with air and bottom with substrate. Due to faceted grain formation at low temperature the mismatch between adjacent grain will be lowerer at middle compare to top where air contact have due to surface tension reason. During growth of nucleation by process of 2D nucleation, material will flow through this area and result in abnormal grain by expense of smaller grains. And the top of smaller grain surface will move and will cover the surface of big grain. At high temperature just below roughening transition temperature the mark of faceted grain on big grain will be vanished.

Grain boundary play an important role in every types of properties of material such as conductivity, creep resistance, fatigue, corrosion resistivity etc. Grain boundary surface tension analysis can solve some problem.

C. Types of Grain boundary

1.General grain boundary

It is impossible to draw this type of grain boundary in atomic point of view due to high degree of disorder.

2.Special grain boundary

Various types of special grain boundary have. Among that Low angle grain boundary and CSL grain boundary are described here.

a. Low angle grain boundary

Low angle grain boundary is not actual grain boundary because it may be found into grain as sub grain boundary.

b. CSL(coincidence site lattice) boundary

In section 2.6 further illustration about CSL grain boundary has been given. However, here below is given a clear picture to know about what is coincidence site.

During rotation of two sheet of 2D lattice for certain angle the fraction of overlapping sites will be increased for certain angles. The grain boundary that contains such coincidence sites are called CSL grain boundary. In 3D view the boundary will be looked similar but should have different tilt axis.

According to the fig. 3, corner atom of top sheet share 4 neighbouring sites and side atom share two neighbouring sites. So

Total site atom of top sheet 70 + 7 +10 + 1 = 88.
Among that 14 + 7/2 = 17.5 sites coincide. So, the sigma value will be reciprocal of coincidence sites percent.

$\Sigma = 1/(17.5/88) = 5.0285 = 5$ (approximate)

So, for higher value of sigma coincidence sites will be lowerer and the top sheet will be then less common sites with bottom sheet, in other words then the top grain will be

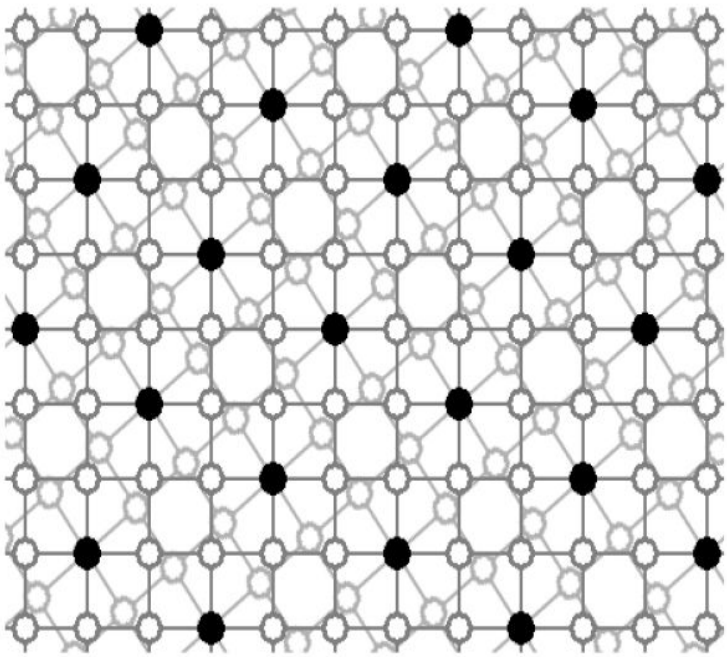

Fig. 3. 2-dimensional illustration of CSL principle. Two interpenetrating lattices are shown, the lighter turned 36.78 degree anticlockwise with respect to dark lattice. Coincident site position are marked with black.[1]

isolated more from the bottom grain. Approximately, no matching will not be then observed between this two grain. The potential barrier between grain for high sigma value will be then large.

4. Twin boundary

Across twin boundary, the regular stacking sequence of closed packed plane {111} is inverted from ABC ABC .. to ACBACB .. creating a narrow band of hexagonal closed packed structure (around the twining plane). Twin boundary is an indication of grain boundary dissociation.

D. Herring-Wulff Theory

Herring and Wulff depveloped separately a relation between shape of particle change according to changes of surface tension along different crystallographic directions. According to modern mathematical perspective the proof of Herring-Wulff Theory[28] is very complex.

1. Smooth interface vs Rough interface

To represent same kind of surface either smooth or rough, different articles highlighted different words. To eliminate confusion ,reader are advised to look up on table 1.

Fig. 4. gives a good example in perspective of view "what is smooth surface?" and "What is roughen surface?".

It is noted here if terrace, ledge and kinks are present on surface more, then in micro scale it will be looked smooth surface due to resolution effect. In crystal growth, smooth and rough terms are preserved for atomic scale smooth and rough. And we know typical atomic dia is in nono scale.

2. Identification of crystallographic plane on structure.

Crystal that follow strong periodic bond chain (PBC) during growth that will show flat (F), stepped (s) and kinked (K) faces as like Fig. 5.

Table 1. Different Notations to represent Surface of Crystal [1]

author of paper	term use to refer two types of plane	
kossel, stranski	complete plane	incomplete plane
burton, cabrera, frank	singular interface	non-singular interface
hartman, perdok	F face	S and K face
present	smooth interface/ complete planes	rough interface/ incomplete planes

3. Relationship between crystal shape and gama plot

The problem of determining the equilibrium shape of perfect crystal was proposed and first solved by wulff in 1901. In nature this ideal “wulff shape” (Fig. 6) is observed in crystals that are small enough to relax to their lowest energy state without becoming stuck in local minima.

The wulff problem is to determine the equilibrium shape of a perfect crystal of one material in contact with a single surrounding medium. The equilibrium shape is determined by minimizing the total system energy, which is composed of contributions from the bulk and surface of the crystal. If we consider a fixed volume of material, the bulk energy is also fixed and the problem becomes that of finding a shape of given volume with minimal surface energy.

If the surface energy density –that is , the “surface tension” – is constant, the solution is

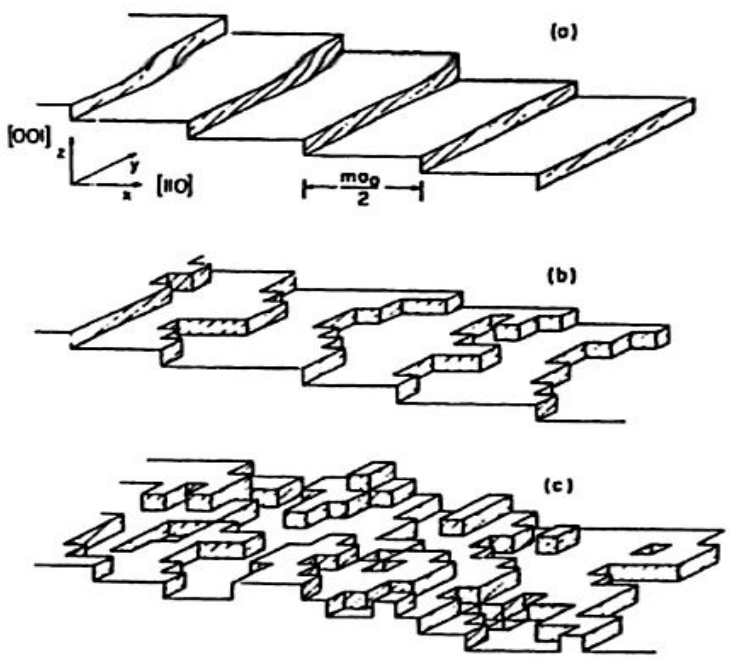

Fig. 4. Typical example of (a) Smooth (b) Smooth to rough transition (c) Roughen Surface. (According to TLK model of crystal interface)

the shape of minimal surface area, which is a circle in 2D and sphere in 3D. However, in many solid materials the surface tension depends on how the surface is directed relative to the bulk crystalline lattice due to the detailed structure of the bonding between atoms. Assuming some standard orientation of the bulk lattice, the surface tension γ will be a definite function of the normal vector to the surface say γ = γ (n^). In that case if the material is bounded by a surface Γ the total surface energy is surface intrigal

$$E = \int_{\Gamma} \gamma(\hat{n}) dA, \tag{1}$$

if $\hat{n} = \frac{\nabla \phi}{|\nabla \phi|}$, $dA = \delta(\phi)|\nabla \phi| dx$ then

$$E(\phi) = \int \gamma(\frac{\nabla \phi}{|\nabla \phi|}) \delta(\phi) |\nabla \phi| dx \tag{2}$$

Which must be minimized subject to the constraint of constant volume enclosed by Γ . This problem makes sense both in two and three dimensions and essentially 2D crystals do arise experimentally in the growth of thin films.

When solid crystal from liquid the first nuclei will be circular shape but as it grows it will make wulff crystal shape. The total surface energy will be lower as it grows. The surface energy and volume ratio can be calculated from the following equation

$$\frac{E}{V^{1-1/d}} = \frac{\int \gamma(\frac{\nabla \phi}{|\nabla \phi|}) \delta(\phi) |\nabla \phi| dx}{\int H(-\phi) dx} \tag{3}$$

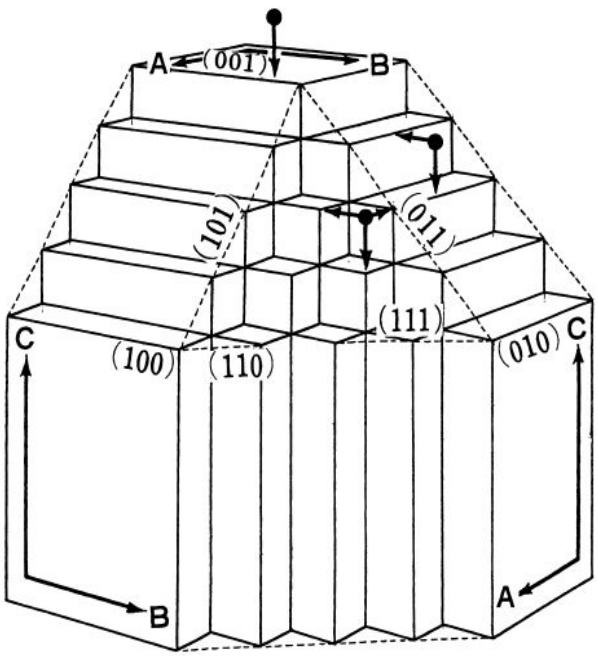

Fig. 5. PBCs and F, S, K faces defined in Hartman-Perdok model. Thick lines with arrows, A, B and C are PBC vectors in a simple cubic crystal Kossel crystal, F faces: (100), (010), (001), S faces: (110), (011), (101), K face: (111). [1]

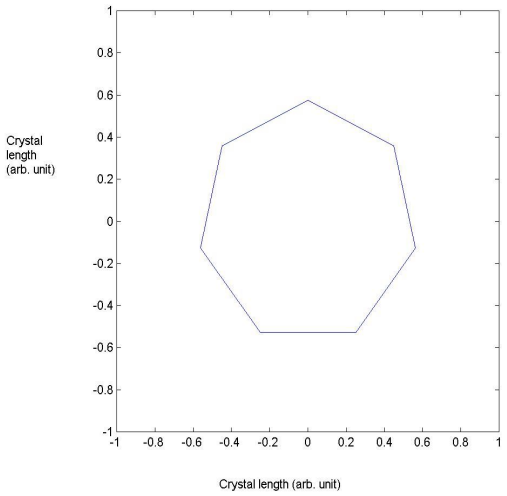

(a)

(b)

Fig. 6. (a) A 2D Wulff crystal. (b) A 3D Wulff crystal

1. Improtant Notes on ‘d’

‘d’ is the dimension. For two dimensional crystal, crystal will be surrounded by line then d=2. And for three dimensional crystal, crystal will be surrounded by surface then d=3.

2. Important notes on ‘x’

x is the trajectory on particle interface.

3. Important notes of ‘ϕ’

‘ϕ’ is called set function. This auxiliary function can be consider as kind of trajectory but it’s value is defined such that it will be less than zero if it is a member of omega Ω, will be zero if it is member of gama Γ, otherwise it will be greater than zero.

4. Important notes on ‘δ’

It is a one dimensional delta function. It point out for certain growth direction; about what, we are concentrated for that time.

5. Important notes on ‘H’

‘H’ is a one dimensional Heaviside function. This term comes for three dimensional wulff plot analysis.

if we consider ε = 3 dx ,then

$$\delta(\phi) = \begin{cases} 0 & \text{if } \phi>\varepsilon \\ -\frac{1}{6\epsilon}(1+\cos(\frac{\pi x}{\epsilon})) & \\ -\frac{1}{6\epsilon}(1+\cos(\frac{\pi x}{\epsilon})) + \frac{4}{3\epsilon}(1+\cos(\frac{2\pi x}{\epsilon})) & \text{if } \phi>\varepsilon/2 \\ & \text{Otherwise} \end{cases} \quad (4)$$

$$H(\phi) = \begin{cases} 0 & \text{if } \phi<=-\varepsilon \\ -\frac{1}{6}(1+\frac{x}{\epsilon}+\frac{1}{\pi}\sin(\frac{\pi x}{\epsilon})) & \text{if } \phi<=-\varepsilon/2 \\ -\frac{1}{6}(1+\frac{x}{\epsilon}+\frac{1}{\pi}\sin(\frac{\pi x}{\epsilon})) + \frac{1}{3}(2+\frac{4x}{\epsilon}+\frac{1}{\pi}\sin(\frac{2\pi x}{\epsilon})) & \text{if } \phi<=\varepsilon/2 \\ -\frac{1}{6}(1+\frac{x}{\epsilon}+\frac{1}{\pi}\sin(\frac{\pi x}{\epsilon})) + \frac{4}{3} & \text{if } x<=\varepsilon \\ 1 & \text{Otherwise} \end{cases} \quad (5)$$

We know in solid case, for one dimensional lattice, surface tension is a summation of

cosine and sine functions. Cosine term arises for terrace and sine term arises for ledge in crystal. That means surface tension will be change as the angle between planes changes in solid state. However, for triangular wulff shape formation in 2D , surface tension can be approximated as

$$\gamma(\nu) = 1 + \left|\sin\left(\frac{3}{2}\left(\nu + \frac{\pi}{2}\right)\right)\right|. \tag{6}$$

By putting the surface tension equation in energy equation we can measure surface energy.

Wulff's geometric construction described above can be mathematically formalized by the use of the legendre transformation, which we define below.

Definition 1 Let Zeta $\zeta : S^{d-1} \rightarrow R^{+}$ be a continuous function.

1. The first legendre transformation of Zeta , ζ is

$$\zeta_*(\nu) = \inf_{\substack{\theta \cdot \nu > 0 \\ |\theta|=1}} \left[\frac{\zeta(\theta)}{(\theta \cdot \nu)}\right] \tag{7}$$

2. The second legendre transformation of Zeta , ζ is:

$$\zeta^*(\nu) = \sup_{\substack{\theta \cdot \nu > 0 \\ |\theta|=1}} \left[\zeta(\theta)(\theta \cdot \nu)\right] \tag{8}$$

The geometric interpretation of legendre transformation should be clear from Fig. 7.

Here below is given an example to find out wulff shape function from given surface tension function by process of legendre transformation.

In 2D the surface tension function 'γ' is usually given in term of angle 'ν' of normal $\hat{n}$ to a fixed horizontal axis i.e. γ =γ(ν). We extend γ as a homogeneous function of degree one in the following way.

And easily we can get

$$\gamma_*(\theta)\hat{n}(\theta) = D\gamma(\nu) = \gamma(\nu)\hat{n}(\nu) + \gamma'(\nu)\hat{\tau}(\nu) \tag{9}$$

Where

$$\begin{aligned} \hat{n}(\nu) &= (\cos\nu, \sin\nu) \\ \hat{\tau}(\nu) &= (-\sin\nu, \cos\nu) \end{aligned} \tag{10}$$

When γ is convex, that is when

$$\gamma + \gamma'' \geq 0 \tag{11}$$

the top equation is a parameterization of the Wulff shape in term of γ and the legendre transformation of γ is given by

$$\gamma_*(\theta) = \sqrt{\gamma^2(\nu) + \gamma'^2(\nu)} \tag{12}$$

where ν determined by

$$\nu = \theta - \tan^{-1}\left(\frac{\gamma'(\theta)}{\gamma(\theta)}\right) \tag{13}$$

To find the second legendre transformation we extend γ to the whole space as a homogeneous function of degree –1 by defining

From the general relation we obtain

$$\gamma(x, y) = \frac{1}{\sqrt{x^2 + y^2}}\gamma(\tan^{-1}\frac{y}{x}) \tag{14}$$

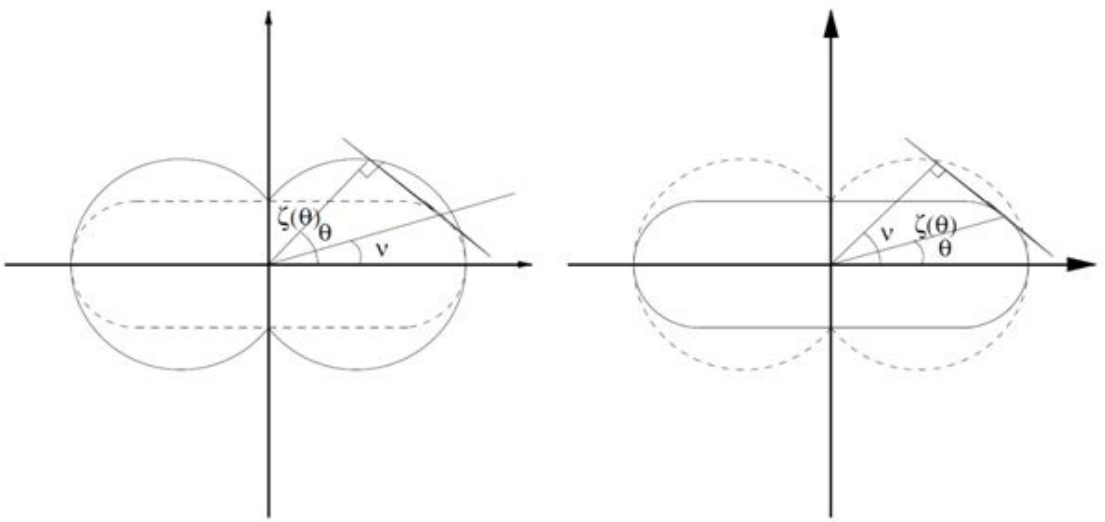

Fig. 7. Left: the first Legendre transformation. The solid line is the plot of ζ, and the dashed line is the plot of ζ_*, the corresponding Wulffshape. Right: second Legendre transformation. The solid line is the plot of ζ, and the dashed line is the plot of ζ^*, the support function.

(15)

$$\gamma^*(\nu)\hat{n}(\nu) = \frac{\gamma^2(\theta)}{\gamma^2(\theta)+\gamma'^2(\theta)}[\gamma(\theta)\hat{n}(\theta) - \gamma'(\theta)\hat{\tau}(\theta)] \quad (16)$$

$$\gamma^*(\nu) = \frac{\gamma^2(\theta)}{\sqrt{\gamma^2(\theta)+\gamma'^2(\theta)}}$$

Where θ is defined by

$$\nu = \theta - \tan^{-1}\left(\frac{\gamma'(\theta)}{\gamma(\theta)}\right) \quad (17)$$

4. Effect of temperature on shape of crystal and ɣ plot

Surface tension will be decreased as we increase the temperature. Fig 8(a) shows that at high temperature the surface tension will be low for a material compare to its state at low temperature. Also at low temperature cups depth in wulff plot will be remarkable but at high temperature just below roughening transition temperature the cups will be removed. The crystal shape will be polyhedral at low temperature but at high temperature above roughening transition temperature it will be circular in 2D. The 8(b) shows a free body diagram of supported particle. Gravitational and surface tension force will be act on particle. The equilibrium shape will not be exact circular. The glass particle interface will not cut the center of particle it will be some what lowerer compare to that position. Also prticle shape will be oval shape due to surface tension effect.

The roughen particle will not show any faceted plane. Faceted pane only will be shown on particle that will be produced below roughening transition temperature. Theoretically roughen particle can be produced above roughening transition temperature and faceted particle can be produced below roughening transition temperature. To retain high temperature structure at low temperature quenching heat treatment one have to do. It is possible to gain faceted structure at any temperature if one flow furnace cooling heat treatment.

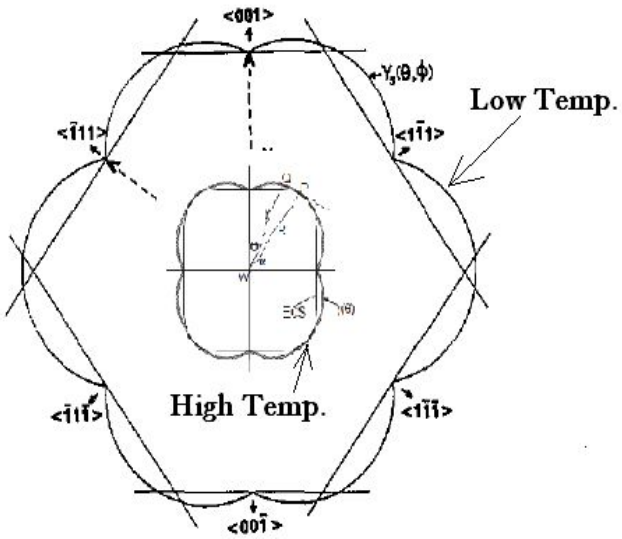

(a)

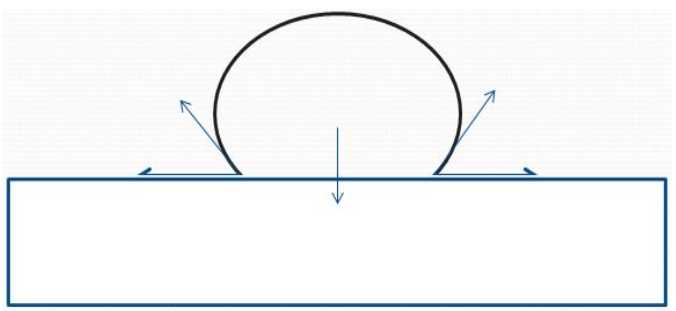

(b)

Fig. 8. (a) Variation of ɣ with temperature of a typical material and different crystal direction.(b) Symantic diagram showing Ag particle on glass.

E. Roughening Transition Temperature (TR)

According to Temkin's result, the interface roughness is not only controlled by alpha-factor (surface tension) but also beta (driving force) and T (temperature). It is seen that smooth interface transform to a rough interface as beta increases. Transform from smooth to rough interface is regarded as a kind of phase transition, so a term "roughening transition" is used. There are "thermodynamic roughening transition" as increasing temperature and "kinetic roughening transition" as increasing driving force.

In this paper, we will determine thermodynamic roughening transition temperature by simplely observing the SEM images of quenced samples. However, it also can be done by observing SEM image of powder that is produced by solution process.

F. Growth behavior

Growth rates are determined by the state of interfaces, the growth mechanism and the driving force. In fig.9. curve a, b, c respectively correspond to the expected growth rate vs driving force relations for spiral, 2DNG and adhesive type growth mechanisms. As the driving force increase according to following figure at first spiral growth should observe then 2D nuclei growth should be observed then 3D nuclei growth should be observed.

The spiral mechanism predominated region or the 2 DNG predominated region depends on crystallographic directions , crystal faces , environmental phase (solid , solution, melt, vapour phases), solute-solvent interaction energies in solution growth (corresponding to solubility difference), as well as size of crystals.

We know dendritic growth is exactly opposite of faceted growth (spiral and 2DNG) because during dendritic growth favorable nucleation site is not on interface it is in front

of interface a little distant far from interface in to melt. Due to rough surface for this kind of dendritic growth, atom added easily we can call it adhesive mechanism. So, for dendritic growth of nuclei is more on surface normal direction. Previously we have said metal with low surface tension will not suitable to retain flat face so it will flow 3D dendritic mechanism. For the same reason, same metal in air environment due to high surface tension will flow 2D nucleation compare to metal in liquid surrounding.

At low temperature and low driving force growth is controlled by spiral growth mechanism. Spiral growth layers advance outward starting from inner portion of a face resulting in macroscopically flat crystal faces. Namely this region is a region where a polyhedral face bounded by flat faces is expected. The normal growth rate of a face in this region is determined by hight of spiral growth layers, step separation and advancing rate of spiral steps. In this case faces with lowerer normal growth rate develop larger compare to faces with higher normal growth rate. Step hight, step separation and advancing rate are three important parameter for spiral growth mechanism. Step hight is determined by lattice spacing, step separation is related to critical radius of 2D nuclei which is related to edge free energy and driving force. Step advancing rate also depends on edge free energy and driving force. Macroscopically spiral growth and 2D nucleation growth is responsible for abnormal grain growth. The reason is then due to low mismatch between adjacent grain, big grain grows with the expense of small grain but due to air contact top surface cover on big grain and at latter stages it remove if we increase temperature.

1. Critical radius and energy barrier for Abnormal grain growth (AGG).

Two-dimensional(2D) nucleation will be discussed here which plays not only an important role in thin-film deposition process but also reflects the bulk crystal growth at atomically flat phase boundaries. It is well known that after the 2D-nucleus is formed, the whole interface plane is then rapidly completed by lateral growth.

The change of the free gibbs potential at the generation of a disc-shaped nucleus is

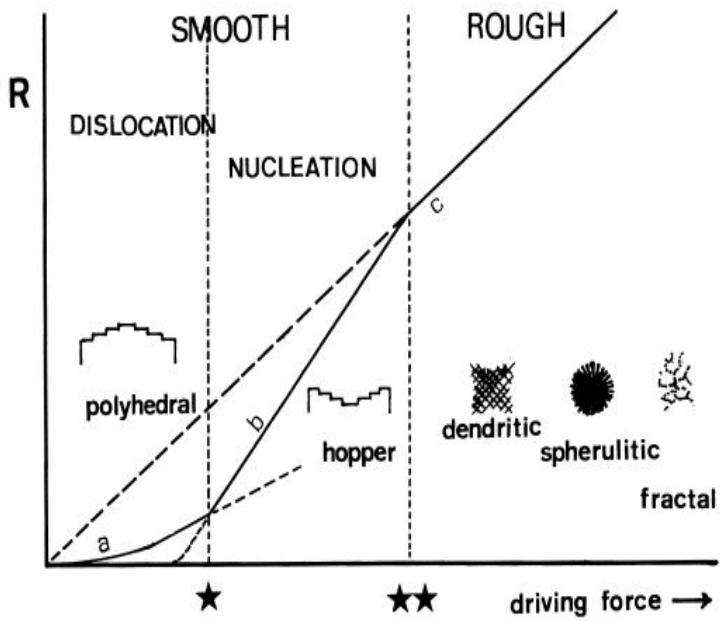

Fig. 9. Schematic illustration of mutual relation among different form of crystals, in relation to growth rates (verticle axis) versus driving force (horizontal axis) relations in three types of growth mechnisms. Curve (a) spiral growth (b) two dimensional nucleation growth mechanism and (c) adhesive type growth mechanism. From ref [1].

expressed by the energy balance

$$\Delta G_{2d} = \Delta G_v + \Delta G_{IF} \quad (18)$$

$$\Delta G_{2d} = -\pi r^2 a\ \Delta\mu/\Omega + 2\pi r a\ \gamma \quad (19)$$

Where ΔG_v associates with increasing volume of the nucleus.

ΔG_{IF} denotes the energy required for increase of nucleus surface.

'r' is the radius of the nucleus disc

'a' lattice constant

'Ω' molecular volume

'γ' surface tension

$\Delta\mu = (\Delta h \Delta T)/T_m$ is the driving force, Δh = Heat of fusion.

The maximum i.e the critical value of ΔG_{2d} at which the nucleus is stable, can be obtained by $\delta(\Delta G_{2d})/\delta r = 0$. Then the critical nucleus radius becomes

$$r^* = \gamma\ \Omega/\Delta\mu \quad (20)$$

Combining equation (1) with equation (2) the critical nucleation energy becomes

$$\Delta G^*_{2d} = (\pi\Omega\gamma^2 a)/\Delta\mu \quad (21)$$

For instance, in the melt growth of the atomically smooth and dislocation-free {111} face of Ag crystals in a very slow cooling process (ΔT = 4 k) the driving force

$\Delta\mu$ = (11.97KJ/mole*4K)/1235K =38.76J/mole

Ω = 10.27cm^3/mole, γ_{ls}=0.11 * 10^4 J/cm^{-2}

So, from equation (2)

r^* = 29 nm.

2. Microstructural evaluation of growth behavior

As we increase the temperature first we will observe neck formation among Ag particles.

(Fig. 10) Then the boundary between particle will be faceted. The surface tension on Ag-air/nitrogen surface will be high compare to surface tension on silver-silver interface. In some portion of silver-silver interface the faceted grain boundary will be removed because to provide sufficient material to grow large grain. More material is needed for bigger grain to grow compare to smaller grain. These abnormal grain growth will flow 2D nucleation and growth mechanism, this nechanism is fully controled by high surface tension in solid state. In this mechanism the grain boundary property will be varied along different crystallographic direction according to wulff plot. And material flow and step growth will be controlled by fully surface tension. At high temperature the grain shape will be roughen.

G. Cubic Coincidence Site Lattice (CSL)

When facet form at grain boundary then some types of super lattice structure was observed at grain boundary. That is the result of ordering. This super lattice structure can be explained by CSL model.

1. Cubic rotation

The relative orientation of two crystals is described by the rotation of one crystal, which brings its crystal axes into parallelism with those of the other crystal. Three independent parameters are needed to define such a rotation. A number of different mathematical notations are available for describing rotations. These notations and the relations are available for describing rotations. For our purposes the two most appropriate notations are: (a) the rotation matrix

$$R = \begin{matrix} a11 & a12 & a13 \\ a21 & a22 & a13 \\ a31 & a32 & a33 \end{matrix} \qquad (22)$$

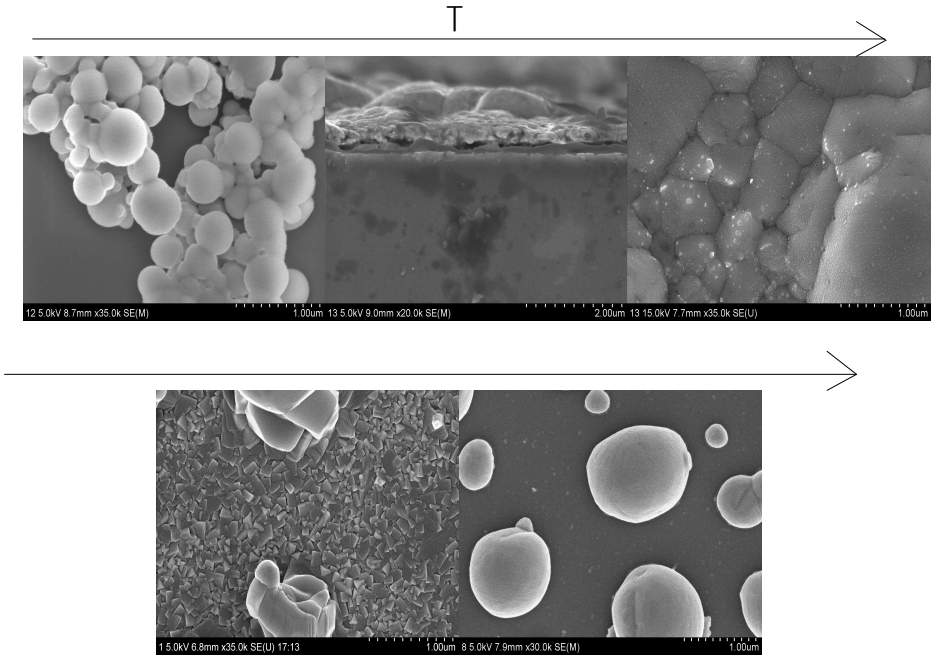

Fig. 10. Microstructural evolution of growth behavior of Ag

Where the aij are column vectors of direction cosines between the cartesian axes.

For simplicity here the rotation matrix for HCP lattice[29] with respect to [001] axis and 21.79 degree rotation is discuss here. Rotation matrix for sigma value 7 in this case is

$$R= \begin{matrix} 8 & -3 & 0 \\ 3 & 5 & 0 \\ 0 & 0 & 7 \end{matrix} \qquad (23)$$

The relative orientation of two cubic crystals can be described in 24 different ways, as the three cube axes are equivalent. By convention, right-handed coordinate systems are used and the right-handed screw direction outward along the rotation axis is the positive rotation direction. Rotation angle θ ,greater than 180 degree about an [h k l] axis are writen as (360 -θ) [-h -k -l] or can be written as (θ - 360) (i.e negative θ) about [h k l]. When the poles of the 24 rotation axes are ploted onto a hemisphere in the stereographic projection, then (in the absence of symmetry) one pole falls in each unit triangle. One of the 24 rotation axes will (in the absence of special symmetry) be associated with the smallest rotation angle θmin .This angle -axis pair is chosen to describe the orientation matrix notation, using the quaternion notation, have determined the range of θmin values. It extends to 45 degree for <100>, to 60 degree for <111>, to 60.72 degree for <110> and has a maximum of 62.80 degree for <1,1,sqrt2 -1>.

2.Cubic Coincidence Site Lattices

When two cubic lattices with the same lattice parameter, which have one lattice point in common, are related by any of a series of special rotations through the common point, they can produce a three-dimensional super-lattice of common lattice points. These are called Coincidence Site Lattices (C.S.L's) and the fraction of lattice points in common is usually written as 1/S, Where S is an odd integer. Cubic C.S.L.'s can be analyzed using rotation matrix formalism. The quaternion notation is much more economical for calculating C.S.L. relations to calculate the number of distinct forms of each C.S.L. and to extend the list of disorientation up to Σ = 57.

For C.S.L.'s of coincidence fraction Σ, the rotation matrix can be written as

$$R = \frac{1}{\Sigma}\begin{bmatrix} A11 & A12 & A13 \\ A21 & A22 & A23 \\ A31 & A32 & A33 \end{bmatrix} \quad (24)$$

and the rotation quaternion as (A,B,C,D) with A2 + B2 + C2 + D2 = Σ : then the Aij and (A,B,C,D) numbers will be integers with no common factors. For Σ > 11 there can be more than one solution to the defining equation: that is. more than one C.S.L. can exist for a given Σ value. As a sort notation to distinguish such C.S.L.'s the letters a,b,c. are added to the Σ number. For example, the three C.S.L's with Σ =33 are labelled 33a, 33b, and 33c, the lowest θmin value takes the letter a, etc. When two C.S.L's have the same θmin and the same Σ , the differentiating letter is given in order of h+k+l, the axis with lowest h+k+l taking priority.

To understand the relation between rotation of one lattice to another[29] we can consider HCP and Cubic cell. Because any rotational hexagonal cell may be chosen from a sublattice of a cubic lattice all rotation leading to any cubic CSL will give rise to a CSL of hexagonal lattice. The latter often however often be a higher value of sigma. Choose for example a hexagonal cell such that

100 hex. = 033 cubic

010 hex. = 3$\bar{3}$3 cubic

001 hex. = 44$\bar{4}$ cubic

Then

$$\Sigma = \begin{bmatrix} 0 & 3 & 4 \\ 3 & -3 & 4 \\ 3 & 0 & -4 \end{bmatrix} \quad (25)$$

$$\Sigma^{-1} = \frac{1}{36}\begin{bmatrix} -4 & 8 & 4 \\ 8 & -4 & 4 \\ 3 & 3 & -3 \end{bmatrix} \quad (26)$$

The hexagonal lattice must gives rise to value of sigma of 36 times that for the same

rotation applied to cubic lattice or an integral factor of this. Thus for cubic sigma = 5 the hexagonal lattice must give sigma as one of 5 10 15 20 30 45 69 90 or 180. Different values will arise as cubic axis of the same form will be parallel to hexagonal axes of different forms.

CSL grain boundary is found in many polycrystalline samples. A polycrystal, as its name indicates, is conformed by many different crystal. Each crystal consists of an ordered three-dimensional arrangement of atoms, which repeats itself, throughly the volume of the crystal. These crystals are also known as grains or crystallities. Because each crystal may possess a different orientation, an interface must be formed between two crystals with different orientations when they come into contact. This interface is called grain boundary. A grain boundary is a very complex structure; its mathematical description requires four parameters in the two-dimensional case and eight parameters in the three dimensional one. These eight parameters can be discriminated in five macroscopic and three microscopic parameters. The macroscopic parameters are respectively, three Euler angles ($\Phi_1\Phi\Phi_2$) which describe the specific orientation difference between adjecent crystals to the grain boundary and two parameters describing the spatial orientation of the grain boundary by means of the normal unit vector to the grain boundary pane $n=(n_1n_2n_3)$ with regard to one of the adjecent grains. So 3 angles and 2 orientation on grain boundary are 5 macroscopic variables. The other three microscopic parameters are given by the three components of the translation vector $t =(t_1t_2t_3)$ of the displacement of one crystal with respect to the other. The intrinsic properties of grain boundary depend on the eight parameters. In particular, the mobility and grain boundary energy are predominantly sensitive to them. Grain boundary can be formed in three ways (1) the two crystal meet and rotate with respect to axis that is perpendicular to grain boundary (twist boundary) (2) the two crystal impinges in to each other because rotation axis is parallel to grain boundary (tilt boundary) (3) combination of these two (asymmetrical tilt grain boundary). For higher rotation angles (θ >15 degree), the number of dislocation can be neglected. The positions of the atoms of a perfect crystals are determined by the minimum of the free energy, the atoms will always occupy those positions that lead to this energetic state of the crystal. For the description of the structure of a high angle grain boundary, we can assume that the atoms in the grain boundary try to lie in these ideal positions (low energetic positions). If we take now two crystal with different spatial orientations and superpose them, it is possible to observe that some atoms of both crystals have the same positions; these points are referred to as coincidence sites.

Due to the periodicity of the crystal lattices of both grains, the coincidence sites show also periodicity. In face, the coincidence sites build also a lattice, which is called Coincidence Site Lattice (CSL). If we compare the density of a CSL with respect to the density of crystal lattice, it is possible to define the parameter sigma as the ratio of volume of elementary cell of CSL and volume of elementary cell of crystal lattice . This parameter defines how similar the CSL and the crystal lattice are. The larger the value of sigma is , the smaller is the number of coincidence sites in the grain boundary and vice versa. For example a grain boundary with sigma =1, can be found, if we consider a grain boundary which is supposedly formed between two crystal with exactly the same spatial orientation, small deviations in the orientation of one of the crystals need to be compensated by the introduction of dislocations. Even with the introduction of dislocations the grain boundary can still be considered to posses an sigma =1 since all lattices nodes, except those of the dislocation cores, are in coincidence sites. This type of case is rarely happened for high angle grain boundary. High angle grain boundary can be treated as small deviations from a nearest CSL. Thus we can apply same rule as applied for low angle grain boundary. In the case of LAGB deviation from nearest CSL need to be compensated by lines of dislocations in between regions of undistorted CSL. These dislocations are called secondary grain boundary dislocations (SGBD) and the boundary between them is the perfect CSL boundary generated by the periodic arrangement of primary lattice dislocations. Burgers vector of SGBD is a translation vector of the displacement shift complete lattice (DSC-lattice). As a result DSC lattice contains all lattice points of both lattices.

To gain good property it is expected to increase the population of special grain boundary,
reduce average grain size, enhance microstructure uniformity and fully randomize crystallographic texture. When CSL lattice form at grain boundary then electrical conductivity increases. So it is expected as we increase the soaking time then conductivity will not increase uniformly it will increase and decrease haphazardly depending upon CSL grain boundary formation.

On the table below the CSL for special grain boundary are shown with geometrical details. The sigma value, rotation angle, rotation axis and planes of mirror are shown for different cubic lattice. It should be noted that as cubic lattice has 24 symmetry so sigma 1 CSL means actually no grain boundary have. As sigma value increases the symmetry

produce will be as like symmetry of its parent cubic crystal. So to understand symmetry element and point groups is also necessary to evolute grain boundary in microstructure.

Table 2. Angle and axis of misorientation, maximum deviation, and twining planes for all CSL (Σ <=29)

Σ	θ	UVW	V_m	Planes of mirror symmetry
3	60	111	6.00	111 211
5	36.87	100	3.92	210 310
7	38.21	111	2.96	321
9	38.94	110	2.40	221 411
11	50.48	110	2.03	311 332
13a	22.62	100	1.76	431
13b	27.80	111	1.76	431
15	48.19	210	1.57	521
17a	28.07	100	1.41	410 530
17b	61.93	221	1.41	322 433
19a	26.53	110	1.29	331 611
19b	46.83	111	1.29	532
21a	21.79	111	1.19	541
21b	44.40	211	1.19	421
23	40.45	311	1.10	631
25a	16.25	100	1.03	430 710
25b	51.68	331	1.03	543
27a	31.58	110	0.96	511 552
27b	35.42	210	0.96	721
29a	43.61	100	0.91	520 730
29b	46.39	221	0.91	432

III. Experimental Details

The silver nanopaste was bought from ANP Company which contains 73%(S1), 78% (S 2) solid content with average particle size of 35 nm. The Ag specimens were made by spin coating on glass using 1:1, ethanol : Ag nanopaste ratio. The specimen produced was heat treated at 60^{o}C to 600^{o}C in different nitrogen and oxygen atmosphere. Fig. 11 shows the typical flow chart of experimental process.

A. Heat treatment cycle.

Fig.12 shows a typical heat-treatment cycle. A heat-treatment cycle consist of three steps: Heating up, Soaking and Cooling down.[32]

In heating up step, specimen is heated at a certain rate to attain desire temperature. High heating rate creates nonuniform structure or can damage specimen. Whereas slow heating rate consume more time for sintering. In soaking step, Specimen is heated at constant temperature for homogenization of microstructure. Soaking step can be divided in to three steps: recovery, recrystalization and grain growth. In recovery process prior heat-treatment effect, cold work effect, hot work effect etc is removed by dislocation movement. In this stage the mechanical property is changed according to dislocation distribution morphology. In recrystalization process extra energy is removed by creating new nucli at grain boundary. The diffusion of atoms and interfacial tension control this process. The microstructure of after recrystalized structure generally consist of very small stress free grain. In grain growth process this grain grows with the expense of smaller grain. The driving force for grain growth process is minimization of grain boundary energy. After grain growth process microstructure consist of large uniform grain. After soaking specimen have to cool down. Cooling can be done in three ways: Furnace cooling, Air cooling and Quenching. In furnace cooing process specimen is cooled into heating chamber without giving energy supply. This is very slow cooling process. In air cooling, specimen is cooled under by hot or cooled air supplied by out side. If we allow the specimen to cooled under still air then it will also be air cooling. The air cooling rate is higher compare to furnace cooling. Cooling by quenching is a first cooling process in which specimen is inserted

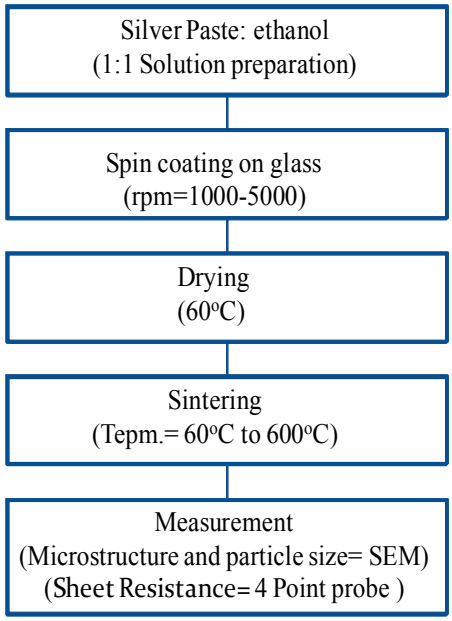

Fig. 11 Flow chart of experimental process

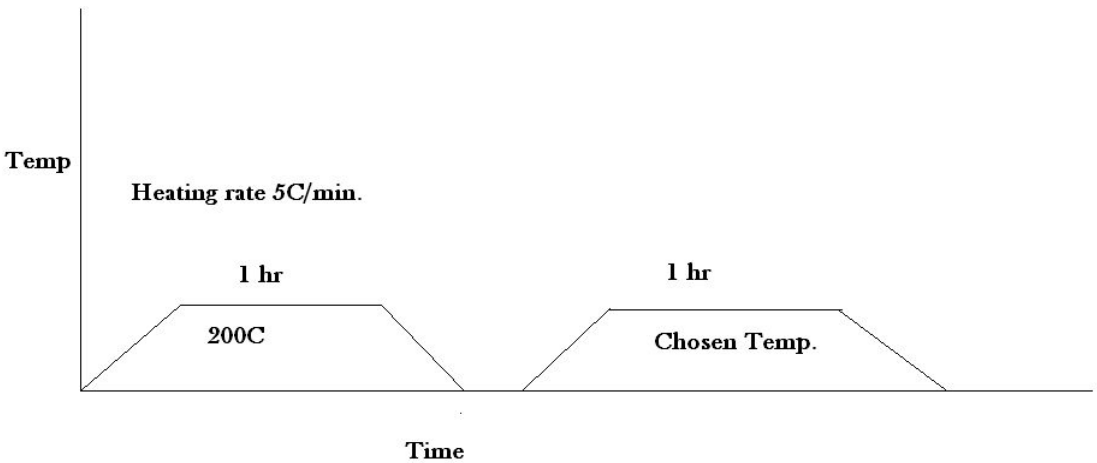

Fig. 12. Heat treatment cycle for investigation of roughening transition temperature of silver nanoparticle

directly into very cooled medium.

Neck growth is the general phenomenon for sintering of nanoparticle [33,34]. The continuity and momentum equation that can be used theoretically to explain growth behavior of silver nanoparticle is:

$$\partial\rho/\partial t + \nabla(\rho\,\mathbf{u}) = 0 \quad (27)$$

$$\partial\mathbf{u}/\partial t + (\mathbf{u}\nabla)\mathbf{u} = \mathbf{F} - 1/\rho\nabla p + \eta/\rho\,\Delta\mathbf{u} \quad (28)$$

Where velocity vector **u**, the pressure P, the density ρ, dynamic viscosity η, additional force F acting on a volume element.

Continuity equation (27) suggest that local density variation is related to change in interface velocity. Momentum equation (28) suggest that interface velocity change also related to change in surface tension and pressure.

I have used double heat-treatment process to sinter silver nanoparticle. A double heat-treatment process is a process in which specimen is soaked two times. Nano particle is very small. To eliminate swelling I have used two time heating instead of one long time heating. Double annealing also helps to remove overheating the specimen.

IV. Results and Discussion

A. DSC (Differential scanning calorimetry) Data for silver

Fig. 13 shows DSC curve of silver nanopaste S1, S2, S3, and S4. It shows that for S1 near 125^{o}C, 275^{o}C, 375^{o}C heat absorbtion were observed and at 200^{o}C and 300^{o}C heat evolution were observed which is 50^{o}C lower than reported[34]. That means after this temperature there has a probability to change surface energy or bonding configuration or order or phase. It is noted here that at 300^{o}C densification didn't observed but at 400^{o}C I observed densification. (Fig. 14). It suggest that may be densification is related to heat

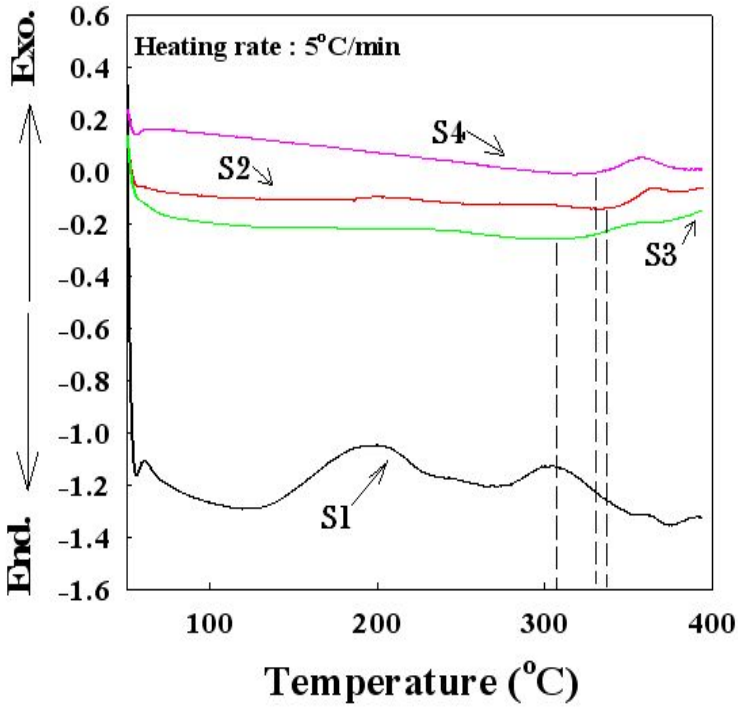

Fig. 13. DSC curve for silver nanopaste

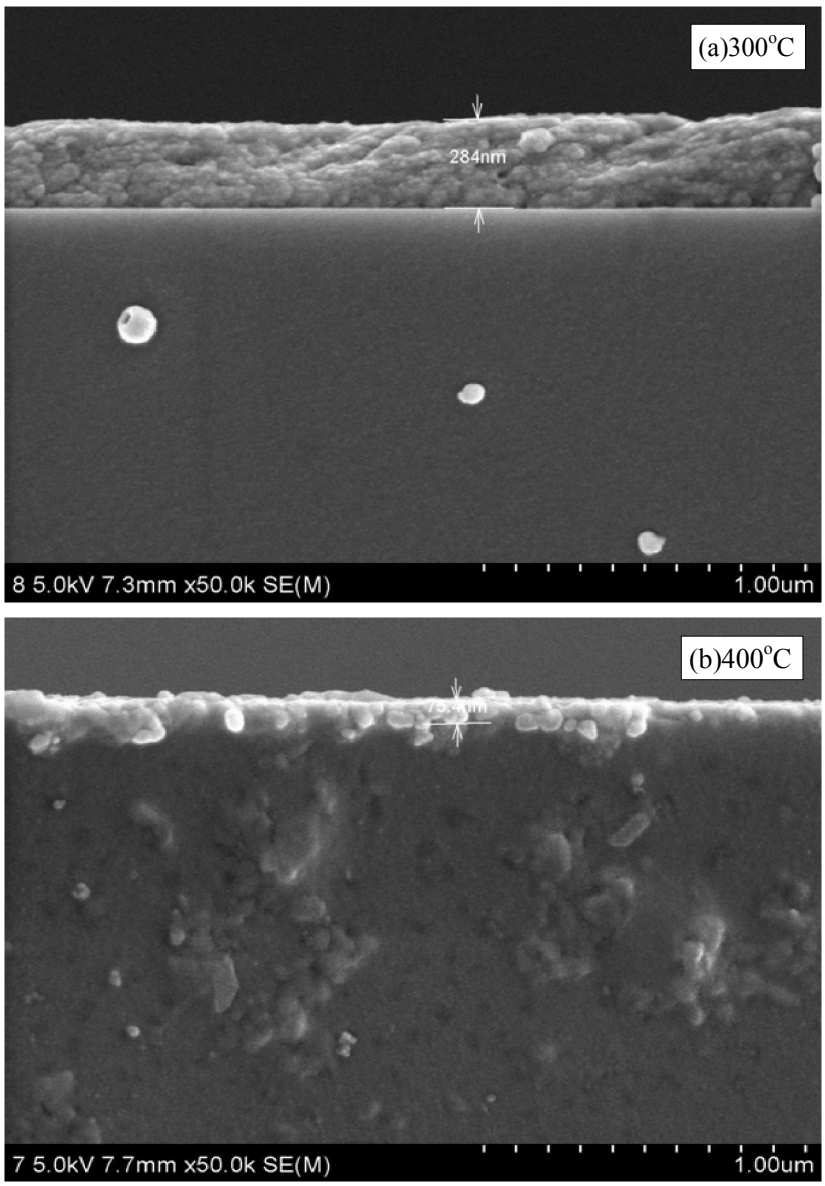

Fig. 14. Densification characteristic observation of silver by SEM (a) 300°C (b) 400°C

removal process. For S2 the particle energy variation temperature was 340^{o}C, for S3 it was 305^{o}C and for S4 it was 335^{o}C.

B. Size distribution of silver nano-particle

Size distribution can be calculated by Matrox Inspector 4.1 Software.[35] Here below is given a graphical representation of size distribution of silver nanoparticle (Fig.15) that has been calculated by Image–J software. It shows that the number of particles between 5 to 15 nm are about 90% but it covers smaller portion of area. Whereas the number of particles between 15 to 45nm are about 9 % but it covers most of the area.

It was observed that most of the space of image of silver nanoparticle was covered by 40 nm particle.

Fig. 16 Shows that before heat-treatment nanoparticles average size was 40 nm (1255 nm^2) but after annealing the Average size increases to 280 nm (61309 nm^2).

To analyze particle shape first I loaded file by file > open command from manu bar of Image J software. Then I drew free hand straight line on scale bar by using free hand straight line draw tool bar. The length of line was exactly as given on SEM figure. Then I went to Analyze > Set scale command on manu bar. Here I put unit of length and known distance according to loaded SEM image. Then I made the image binary by using Process > Binary > make binary command from manu bar. Then all particle changed their shape that only contained black and white colour. The analysis of particle is the main goal of this process so to do this I went to analyze > analyze particle command on manu bar. Then I changed the show tab on that macro to outline. Then after execution image J program I have gotten summary result. From that result I calculated average particle data from average particle area data.

The procedure described here was a simplistic process to make the data reliable, one have to edit and use other tool to clearly show all particle and their outline. Crop tool can be use to delete unwanted portion of the image. To find standard deviation or other statistical data one have to choose suitable selection tool from macro window during

analysis.The importance of particle size and particle size distribution (PSD) is that it will change sintering characteristic as well as growth morphology of Ag nanoparticle. Small particle with high aspect ration facilitates sintering compare to large particle. PSD also effects on rheology, film gloss, surface area, packing density, aglomeration etc. Electrical and steric barrier is necessary to prevent agglomeration. It is also important to know PSD because it effects on setting time, hiding pigment, the activity of catalist, the sintering shrinkage of metallurgical composition, stability, aesthetics, rate of absorption, total bioavailability. Small nanorange particle shows excelent conductivity, chemical stability and ctalitytic activity. Among all metals silver has highest electrical and thermal conductivity which is dependent on its particle size and shape. Nanoparticle has zero dimension, nanowire has one dimension and nanocube has three dimension. All of them have application in the field of optics and catalysis. Low sintering temperature is important in flexible electronic application.[40] Microsize Ag particle shows similar oxidation characteristic as like nano Ag particle. The difference is nanoparticle are frequently carry surface atom in special local environment so oxydation characteristic may very including high oxydation rate of Ag nanoparticle. Nanoparticle that will be used in catalytic application should have narrow distribution of size and homogenious chemical composition.[41] Different processing root have to fabricate nanoparticle among them micro flow through system is remarkable because the laminar flow of reactant produce narrow nanoparticle size distribution.[41]If we increase flow rate then PSD can be reduced. So PSD of Ag is depend on flow rate in this system and optical property of Ag depend on PSD of Ag nanoparticle. Not only optical but also catalytic property of Ag nanoparticle is dependend on flow rate of reactants. The absorbance of Ag nanoparticle will increase with increasing flow rate due to narrow PSD.[41] If aggregate form then absorption will be increased for higher wavelength. The presence of Ag nanoparticle increase absorption as well as catalytic activity by process of oxydation.[41]. Size distribution of Ag nano particle also effects on sintering temperature. Low sintering temperature is expected because some substrate of flexible OLED have low glass transition temperature such as PET. For Ag on PET sintering temperature of Ag should below glass transition temperature of PET. For small particle size sintering temperature is lower , particle size below 5 nm have a sharp decrease of melting point. However Organic additives increases the curing temperature of Ag paste[42]. Small particle have high electrical resistance compare to large particle again the mixture of small and large particle gives best electrical conductivity compare to separate small or large particle. This is due to filling of void among large particles.

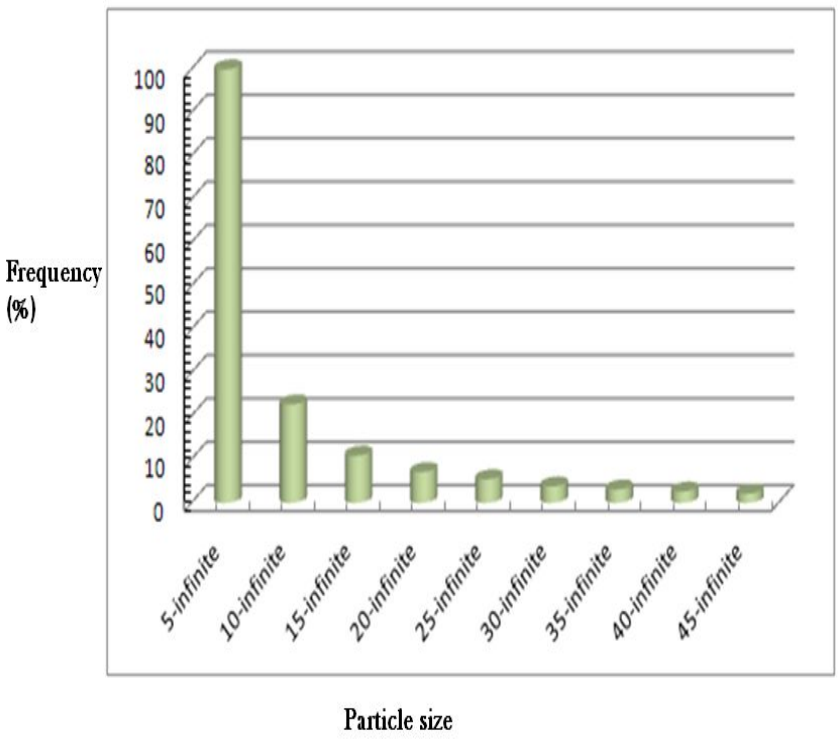

Fig. 15. Particle size (nm) vs frequency (%) graph for silver.

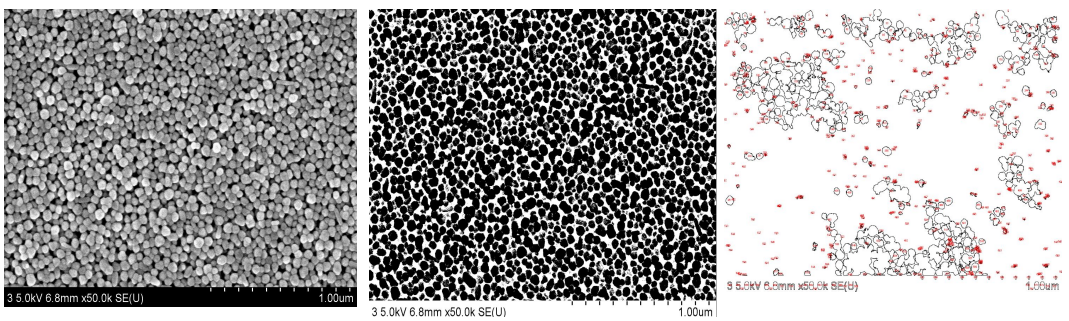

(a)

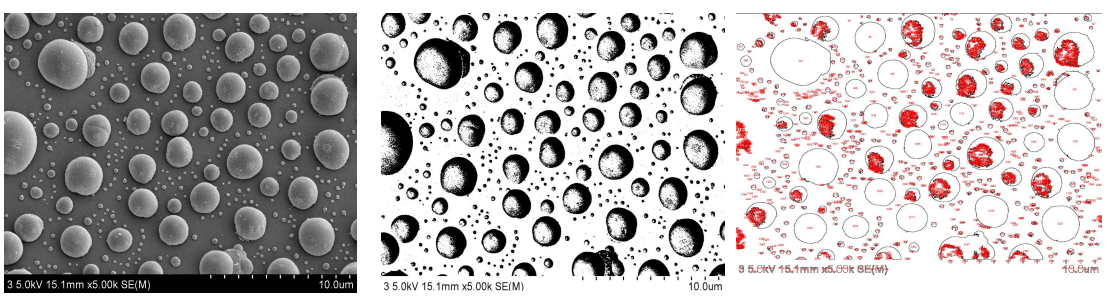

(b)

Fig. 16. Particle size analysis by image J software. (a) green Body (b) quenched at 475^{o}C

C. ADF simulation to construct band diagram of Ag

According to Fig. 19 the conduction band edge of silver is –1.465 Hartree. That means we can consider conduction band above this energy level. It is quite similar as reported[36]. In material, electron flow along certain path and they are bounded by certain plane of crystal. It can be calculated mathematically.[37]

Band diagram construction is an important tool to determine fermi level of any material as well as making comment on work function of material. Generally we know band of material is band of single crystal. But in practical situation defects, grain boundary, dislocation makes the actual band diagram very difficult. Then lots of potential barrier creates in to material. It alter the idle iso energy surface of material. So to describe a property we should be careful about this. If grain size is smaller then potential barrier will be higher then this will increase the conduction band level of material. But special grain boundary have that has low potential barrier then we can find actual band. Band diagram also helps to solve different theoretical problem about the property of material. Fig. 17 shows a image of 40 nm Silver nanoparticle that was constructed using ADF (Amastardum Density Function) simulation.

Input parameters for construction of band diagram of silver are

1. a = lattice parameter = 4.090 Anstron

Primitive vector

2. a1= a/2 x^ + a/2 y^
3. a2= a/2 y^ + a/2 z^
3. a3 = a/2 z^ + a/2 x^

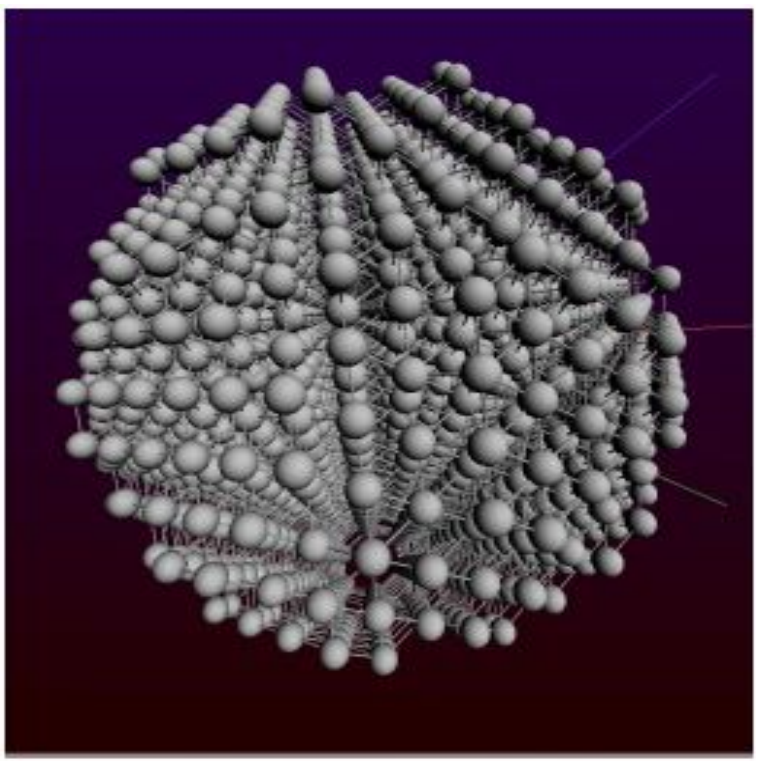

Fig. 17. 40 nm silver nanoparticle

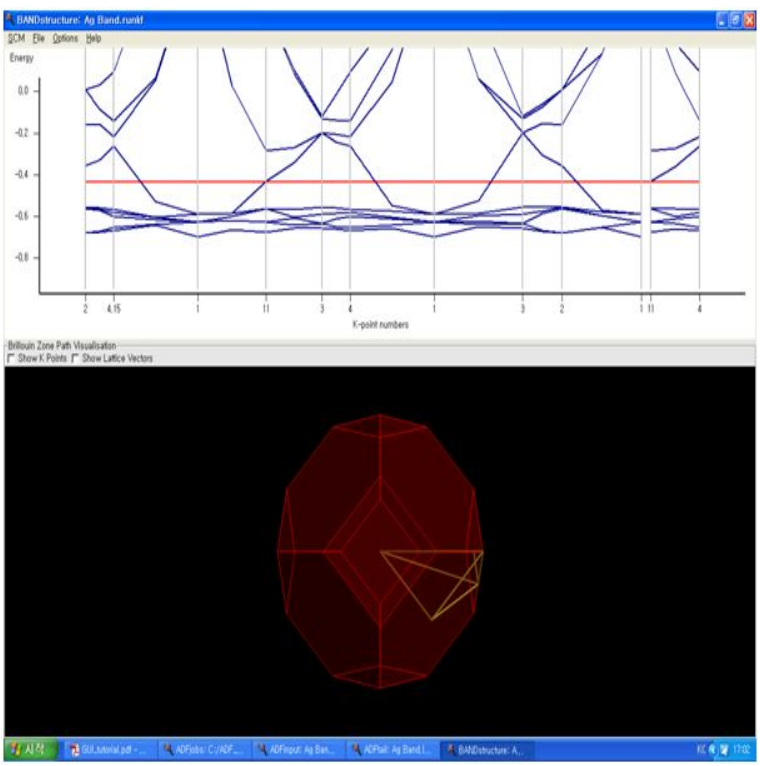

Fig. 18. Band diagram of silver

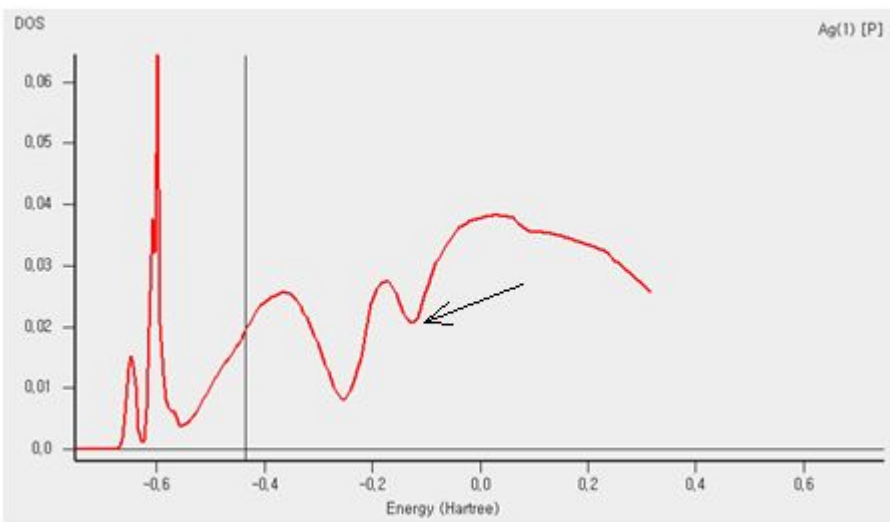

Fig. 19. Conduction band edge of silver

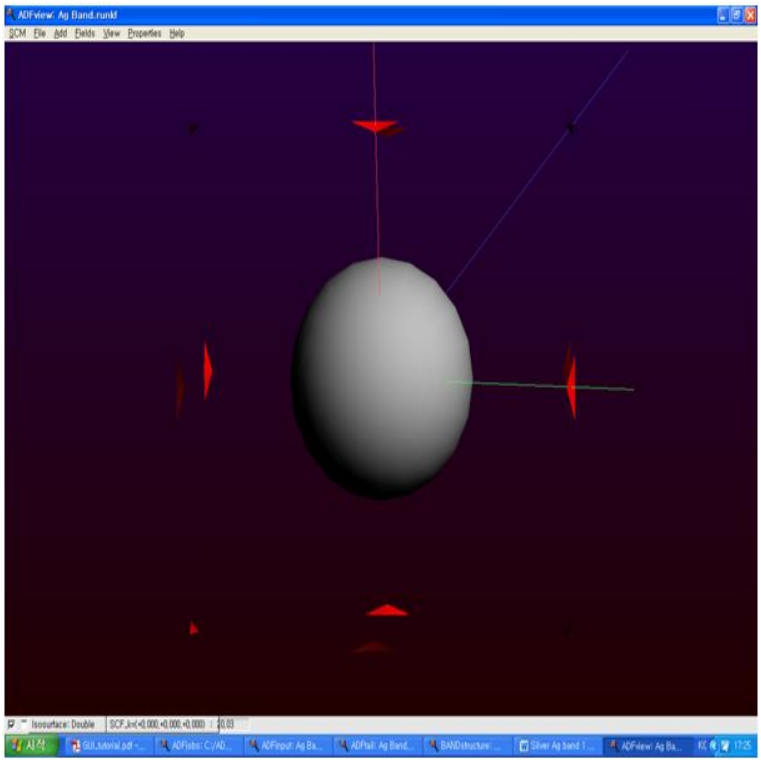

Fig. 20. Constant energy surface for silver at k (0,0,0).

And basis vector = b1 = 0

Band diagram of silver is shown in Fig. 18. valance and conduction band overlap at k=3 represents the metallic characteristic property of silver.

When silver solidifies from liquid then due to electrostatic interaction between silver atoms some constant energy surface (energy level) creates and band structure has been observed. Fig. 20 shows an example of this constant energy surface.

D. SEM images and Rsh value of Ag

We have prepared conductive thin layers of silver on glass of thickness 300 to 1000 nm by spin coating process.

Fig. 21 shown 600 nm thin silver layer sintered at 200^{o}C in N2 . In this case resistance was very low (5.890 Ω/□). We have used nitrogen environment as furnace atmosphere of flow 300 sccm. Spin coating speed was 5000 rpm. Number of layers was two.

During sintering heat flow, sample thickness, prior spin coating speed etc effects on growth behavior of silver nano particle. So conductivity also sometimes vary though the sintering temperature may same. Another reason of conductivity variation is different types of CSL grain boundary formation during sintering. Fig. 22 shows the SEM image of 400 nm thin silver layer with 1.669 Ω/□ sheet resistance, that is produced by using inert argon furnace atmosphere.

By using small starting silver nanoparticles, it is possible to produce more than 1 um last grain size using double annealed method. It is harmfull on property to use more soaking time but it is good to use frequently heating and cooling during heat-treatment of silver nanoparticle. Fig.23. shows a SEM image of silver with 32.5 Ω/□ sheet resistance that is produced by this method.

Fig. 24. shows the last step of removal of faceted grain mark on surface of big particle. Because still there have some faceted mark on surface so resistivity was lower(5.215 Ω/□).

This type of situation can be observed for just below roughening transition temperature of material. Due to initial thickness variation Fig. 23. and Fig. 24. microstructure was completely different. The specimen initial thickness for Fig. 23 was very high.
Fig. 25. shows that rectangular small faceted grain are distributed throughout the structure with sheet resistance 8.549 Ω/□.

As we know from wulff theory during growth by 2D nucleation the first step is the formation of triangular grain then rectangular then pentagon, hexagon, heptagon etc. However it depends on size of nuiclei and temperature of sintering both. So it is possible different types of faceted structure to observe at same sintering temperature but their size must be different. Again temperature gradient through specimen can change the morphology due to nonuniform heat flow.

If we produce multilayer then the quantum well will be formed. Thus due to average band bending the conductivity will be lower compare to single layer. Fig. 26. shows the SEM images of silver thin film that is produced by thinking in mind this kind of effect and it can be applied for practical application as it is suitable in respect of thickness and conductivity.

Fig. 27 shows sheet resistance property variation for different annealing temperature and atmosphere. It was observed that in air and oxygen environment the sheet resistance property din't fluctuate compare to nitrogen sintering environment. However it is expected from CSL concept that sheet resistance property will be nonunifrom with respect to soaking time or temperature.

Fig. 28. shows a graph related to grain size variation with annealing temperature. It showed that as temperature was increased the grain size was also increased. Further more it was observed that in oxygen environment the grain size is larger compare to nitrogen environment. In other words oxygen facilities sintering by removing organic cell by process of oxydation.[34] It also helps to isolate grain from each other.

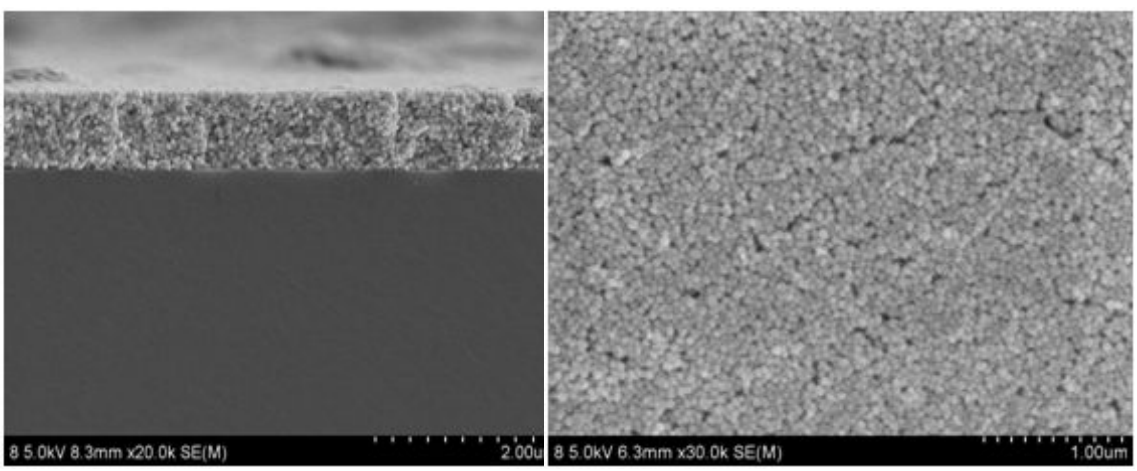

Fig. 21. SEM images of silver nanolayer sintered at 200^{o}C in N_2.

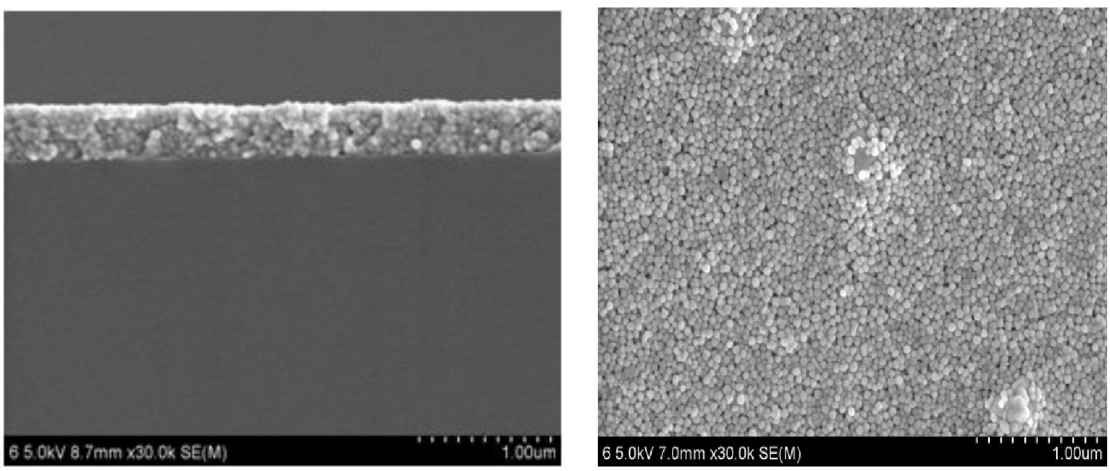

Fig. 22. SEM images of silver nanolayer sintered at 200^{o}C in Ar.

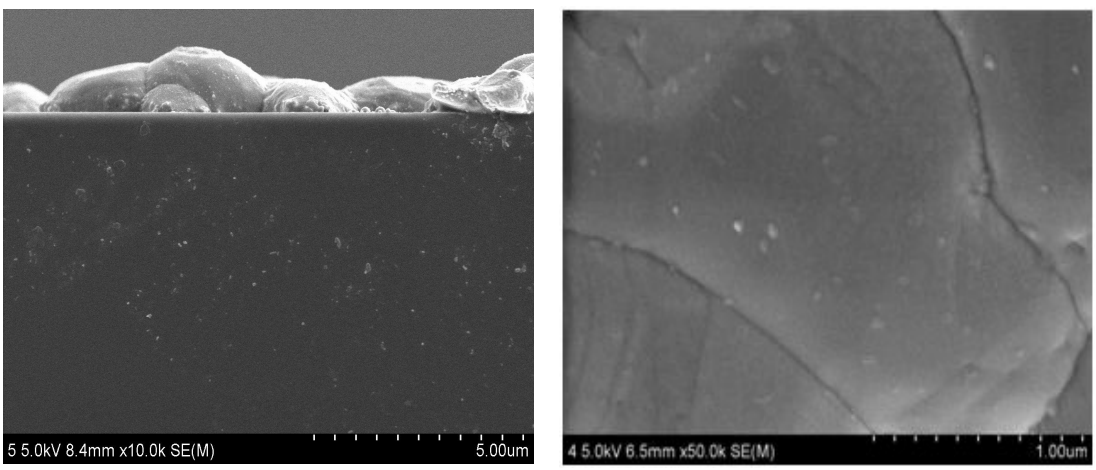

Fig. 23. SEM image of silver annealed at 500^{o}C in N_2 atmosphere.

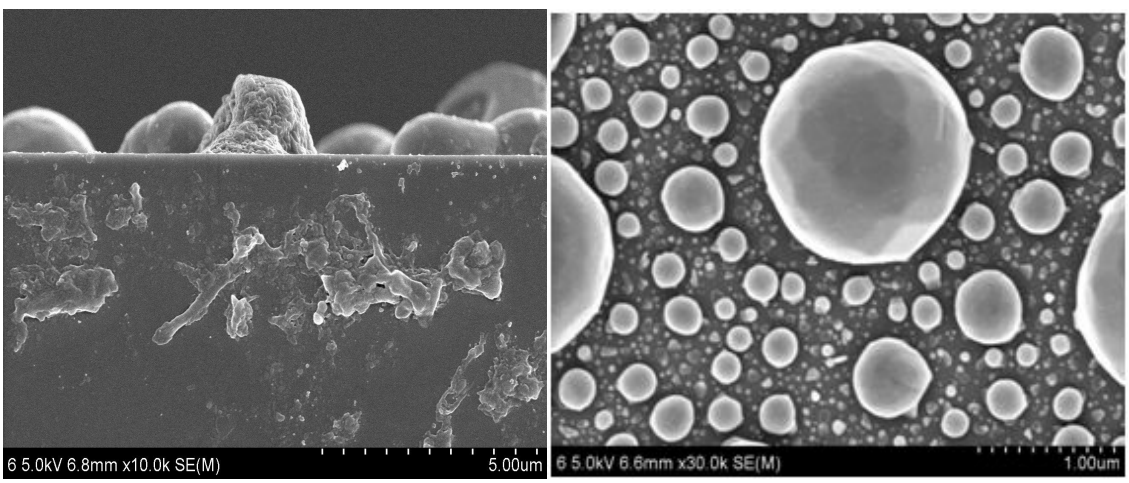

Fig. 24. SEM images of Silver annealed at 500^{o}C in N_2 atmosphere.

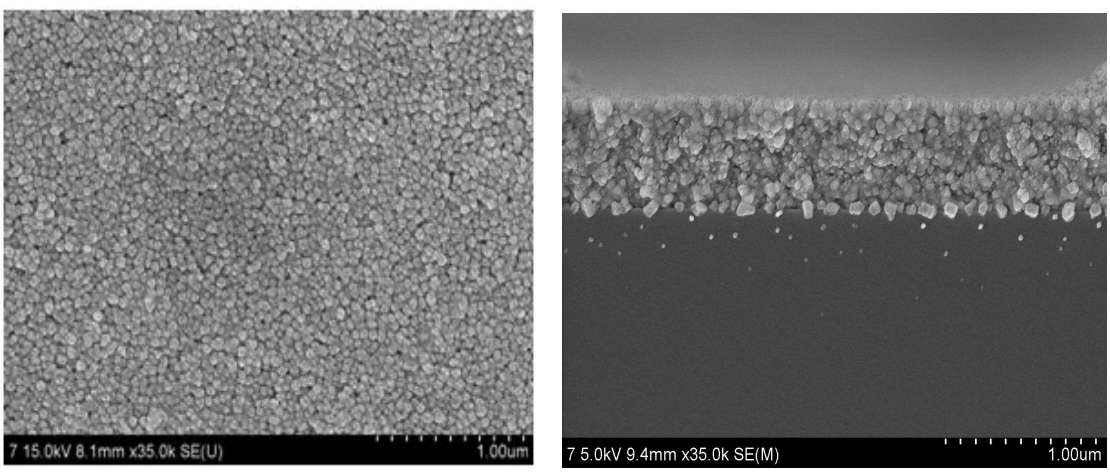

Fig. 25. SEM images of silver annealed at 200^{o}C in N_2 atmosphere.

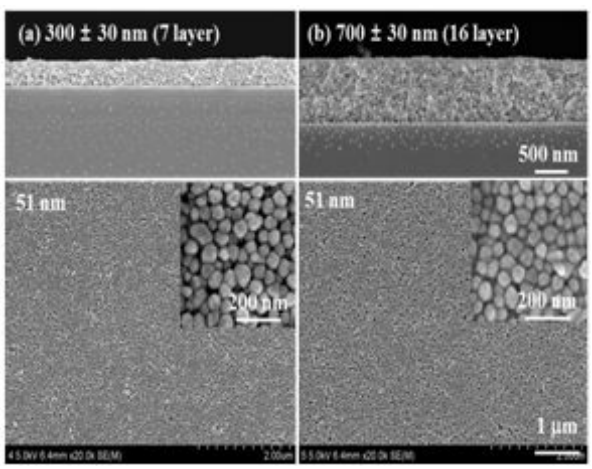

Fig. 26. SEM images of silver nanolayer fabricated by spin coating .

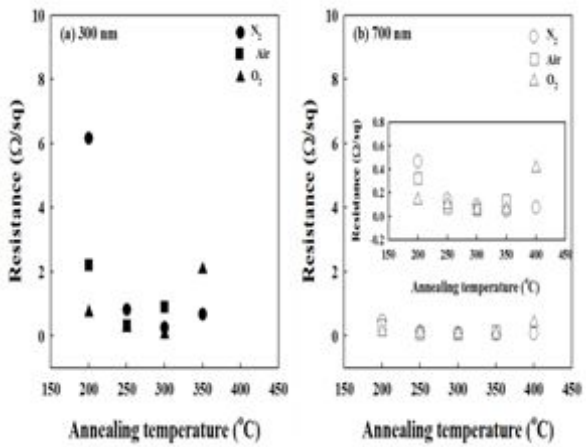

Fig. 27. Sheet resistance variations with annealing temperature and thickness of silver thin film.

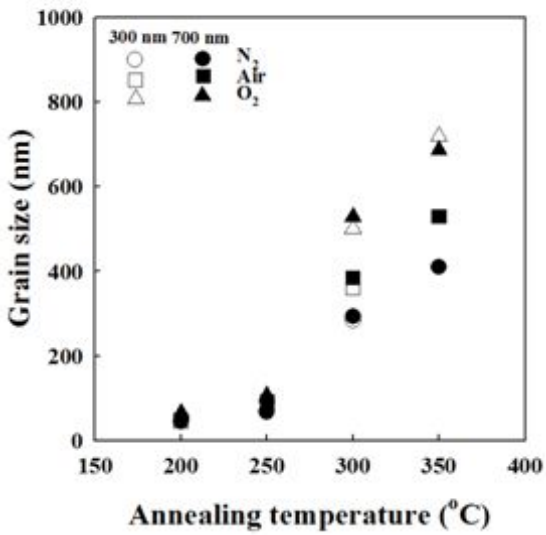

Fig. 28. Grain size variation of silver thin film for different annealing temperature and atmosphere.

E. Different kinds of faceting

Solid phase have high surface tension compare to liquid phase. Again material in solid form for certain closest pack plane shows lowerer surface tension compare to other direction. Anisotropy in the surface energy leads to faceting. This faceting behavior is generally observed for high surface tension material. Then if a faceted surface form then it is difficult to form rounded shape. Silver is a metal that has surface tension which is not too low and not too high. So faceting phenomena of silver is difficult to evolute. Fig. 29,30,31,32,33,34 shows SEM pictures those contain some examples of faceted surface formation for silver. This low temperature structure can formed during furnace cooling of sample from any temperature or by using Quenching from below roughening transition temperature.

We know if F-face produce on structure then we will observe {100} family plane on structure and S-face produce on structure then we will observe {110} family plane on structure and if K-face produce on structure then we will observed {111} family plane on structure.

In Fig. 29 we observe a big abnormal grain on which there have faceted plane and s-face. According to rule this F-face will be {100} family plane. During abnormal grain growth variable grain boundary energy and mobility should observe[38].During normal grain growth all grain boundaries are mobile and size distribution remains uniform. In AGG grain boundary movement is restricted and grain growth proceeds non-uniformly by the growth of few grains , the abnormal grains. At very low temperature abnormal grain growth is not expected. The region of temperature at where abnormal grain growth should observe is between no grain growth temperature and normal grain growth temperature. Abnormal grain growth will be observed below roughening transition temperature and above which normal grain growth should observe. However it also depend on soaking time also[39].It is expected that the abnormal to normal grain growth transition temperature will be increase with soaking time. During growth a curve boundary typically migrate towards its center of curvature and if three grain meet at point then during growth more acute angle grain consume first. In order to abnormal grain growth to occur the abnormal grains must posses some advantage over their competitors such as high grain boundary energy, local high grain boundary mobility, favorable texture or lower local second phase particle density.

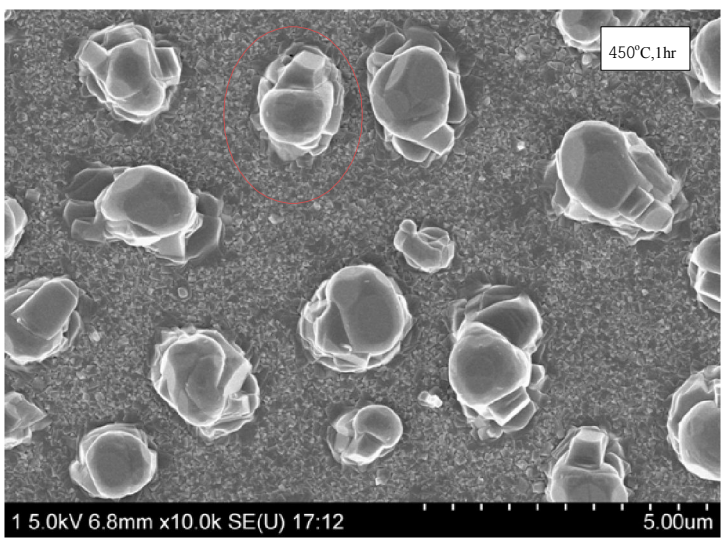

Fig. 29. Abnormal grain growth (island structure) behavior of Ag sintered at 450°C for 1 hr in N2

For low driving force we will generally observe spiral grain. The step of spiral also depends on many factor such as material, sintering temperature, nuclei size, soaking time, cooling behavior, lattice constant etc. Fig. 30 shows a low temperature spiral growth phenomena of Ag. It should be noted here that if we observed faceted structure on microstructure then low temperature structure can be found easily by using high soaking temperature then alow to cool by furnace cooling. Then during cooling grain will be changed their surface according to equilibrium structure.

Each spiral consist of many terraces and ledges that wind around a central screw dislocation. The terrace width are on the order of 10-100 nm where the step hight are one unit cell (1 nm) [43]. The spiral growth structure sometimes looks like wedding cake and cone structure. During cone formation vertical velocity will be equal then grain boundary will not move. In this case grain boundary may or may not straight. If the vertical velocity is not equal then one cone will be largest and it will consume other smaller cone. In true spiral growth step hight is not constant but in wedding cake like spiral growth step hight is constant. Wedding cake spiral growth posses small flat plateaus at the top, a slope (or step spacing) that varies non-monotonically with the distance from spiral core and they are typically separeted by step grooves. These shapes are strikingly reminiscent of the mound structures, it form during the growth of dislocation free metal surface.[44]. However Fig. 30 shows that the spiral structure is tending to vanish because the structure is produced just below roughening transition temperature. Step properties depends on step stiffness or surface tension, and equilibrium atom concentration. A screw dislocation will be shifted during growth so an angle will form around dislocation core. If there have no edge barrier then true spiral growth will be converted to wedding cake spiral growth. That generally shows flat top structure. Growth of wedding cake is governed by two dimensional nucleation of islands on the top of the terrace, which is enhanced by the confinement of atoms due to step edge barrier. Atoms near the top of the spiral mound can avoid the step edge barrier by moving around the core ,which should reduce the local add atom concentration and hence growth rate. On the other hand the indelible presence of step emanating from screw dislocation obviates the need for two dimensional nucleation, which should increase the rate of vertical growth. When the add atom will be sufficiently large so that islands nucleated deterministically, spiral mounds were generally seen to grow higher than regular wedding cake.[44]

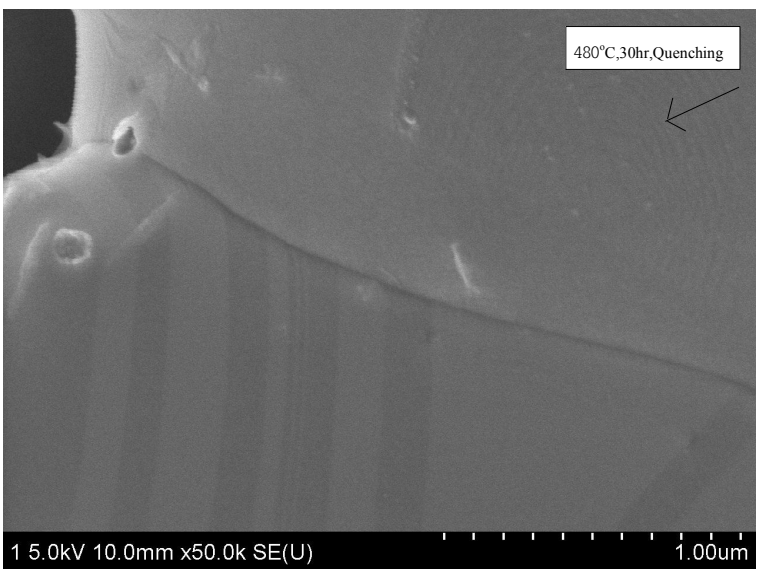

Fig. 30. Spiral grain growth behavior of Ag sintered at 480°C for 30 hr in N2

Step hight will be lower if lattice parameter of material will be lower also it will be lower as the driving force increases. Fig. 31. shows step like structures that has different step separation. S-face are (110) faces of sodium choloride crystal. In this case crystal face is parallel to one most dense row of atoms only it intersect other one and all chemical bonds parallel to latter become unsaturated. So 2D growth sites of S-face is higher compare to F-face but lower than K-face. So normal growth perpendicular to S-face is higher compare to F-face but lower compare K-face. So S-face should form some steps and it property depends on this 2D growth rate. Thus S-face will be disappear first compare to F-face to cease growth. It should be noted here that vicinal surface also offer step growth that depends on cutting of vicinal face of wafer. In this case step length generally is very high that depends on angle of cutting of wafer with respect to particular face. The reason for formation of macro step may be hindrance of step-3 process of spiral growth mechanism due to critical nuclei size don't form and continue step1 to 3 frequently. So now it is necessary to illustrate spiral growth mechanism in detail. Spiral growth mechanism is 4 step process. Step-1: Creation of Screw dislocation. Through center of screw dislocation, dislocation line pass and burger's vector will be lie on distortion plane and it will be parallel to dislocation line. At the end of screw dislocation the length of burger's vector will be one atomic space. Step 2: Second step will be generate that will be perpendicular to the previous step. But if this step length is more than critical length then step-3 will be started. Of course this step advancement depends on concentration of add atoms and other thermodynamic parameters. Step-3: As step-1 helps to form step-2, like this step-2 will helps to generate step-3 if the critical length is achieved. The property of step-3 is similar to step-1 but form at other side. Step-4: As like before step-3 will helps to generate step-4. Thus a round layer of atoms layer will be added that will be look like screw.[45] Second type of spiral growth (wedding cake) step length will be higher and don't form slope. Because here surface tension is higher compare to first type of spiral growth. It will not look like spiral but stacking of smaller circular plate on bigger plate. Third type of spiral growth will be look like cone here step length is very small. In some case one cone consume smaller cone. Forth type of spiral growth is Interlaced spirals. This are the results of the periodic stacking of differently oriented growth layers, each having a different lateral anisotropy of step velocity. Here a step with unit cell may dissociate in sub steps symmetrically related but crystalographically different. The dissociation is the result of different growth anisotropy by each step due to different crystallography. Here one sided growth velocity is equal to the growth velocity of another side of bottom layer.[45]

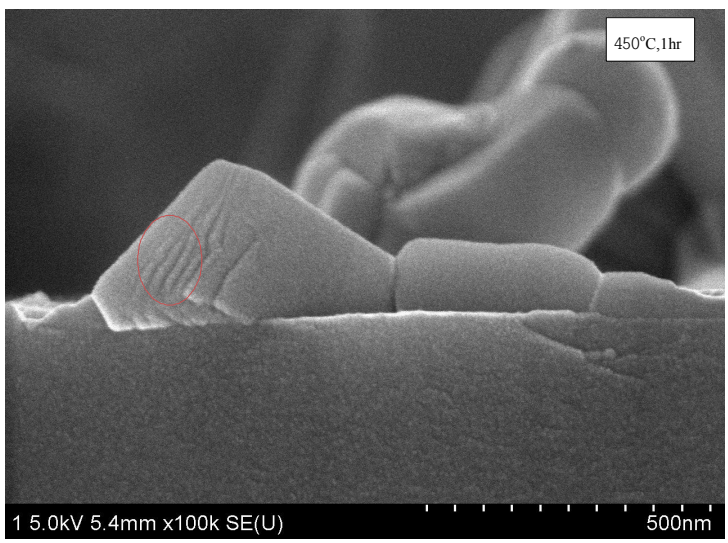

Fig. 31. Step growth behavior of Ag sintered at 450°C, 1 hr in N2

Twining can be consider as thin hexagonal phase in fcc material. This type of faceting some times form angle with each other and can be observed near grain boundary. If it forms then it is difficult to remove twining structure by using heat-treatment process. Grain boundary dissociation sometimes can form twin boundary. Fig. 32. shows twin structure formation on silver grain. Twining is some time expected to remove intergranular corrosion. The annealing twining is not a part of the grain boundary network. Annealing twin will change grain boundary though annealing twin is inside the grain. That is the grain boundary orientation will be changed according to annealing twin. This grain boundaries will be then CSL grain boundaries. The annealing twin generally generate sigma 3 CSL grain boundaries. Annealing twins are symmetrical tilt interfaces on the {111} boundary plane. The twins and sigma 3 boundaries have the same misorientation 60 degree/{111}. Coherent twin boundaries almost immobile whereas incoherent twin or tilt and twist have high mobility. Annealing twin plays central role for stacking low fault energy material. Silver is a midium stacking fault energy materials. Different types of twining have. Tensile twin are observed in case that the c-axis of the matrix are inclined to specimen normal direction by an angle larger than 45 degree. Compression twin on the other hand are found in grains whose c-axis is inclined to normal direction by less than 30 degree. The formation of secondary twin is observed in most compression twins. At the intersection of two secondary twins new grains are formed provided that the matrix and twins have common crystallographic rotation axis. These new grains have a specific orientation relation to the matrix grain, characterized by a rotation about an axis close to c-axis. The importance of twining lies in the fact that crystal unfavourably oriented for dislocation slip are rotated so that dislocation slip can contribute to the following deformation. Further importance of effect of twining are the segmentation of large grain and during high temperature deformation dynamic recrystallization at twin boundaries. Microstructure and texture after thermomechanical treatment is strongly depend on twining activity. Despite the importance still a lack of insight into the relation between the activation of different twins and accompanying microstructural evolution. There are two causes for formation of twins during cooling to room temperature after growth: Phase transition and ferro electric switching. Crystal often can only be grown at elevated temperature where they crystallize in another phase of usually higher symmetry than they adopt at room temperature. On cooling below the transition temperature, twin domains are formed whereas the lost symmetry element of mother phase act as twin element (twin laws) relating the twin domain. Twin domains of ferroelectric crystal switch by mechanical stress from one orientation to another.

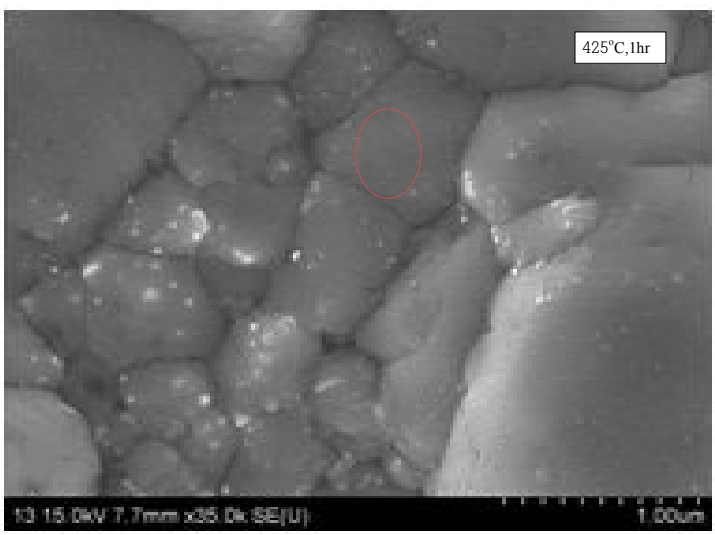

Fig. 32. Twin growth behavior of Ag sintered at 425°C for 1 hr in N2

Different kinds of faceted structures such as triangular, rectangular, pentagonal, hexagonal, heptagonal etc have. But in our experiment we have observed rectangular faceted structures frequently. Fig. 33. shows SEM image of rectangular faceted particle on microstructure. Surface free energy not only depend on temperature but also it depends on local step density. Concern should be taken on that silver change phase 176^{o}C, 571^{o}C, 806^{o}C and 906^{o}C. Supported crystal and activation energy (for growing new layer or dissolving new layer on facet), are two barrier to measure true equilibrium shape. Systematic study of 2D crystal in the form of add atoms and vacancy island on extended flat surface and temperature dependence on shape of 2D islands yields information on the absolute step and kink formation energies of the bounding steps.[46] If wulf plot shows discontinuity at cups then 2D nucleation is expected but if wulf plot change continuously at cups then 3D nucleation is expected[46]. As the step free energy decreases with increasing temperature, it becomes easier to thermally generate new steps. The onset of the surface roughening coincides with this energy becoming zero. Each facet of a certain orientation has its own characteristic roughening transition temperature related to structure of vicinal steps. Crystal growth is difficult on a perfect terrace, and substantial supersaturation is required. When growth does occur it proceeds through nucleation and growth stage, with monolayer thick island having to be nucleated before growth can proceed. A ledge or step on the surface captures arriving atom within the zone of width either side of step. If there are only individual steps running across the terrace then this will eventually grow out and resulting terrace will grow much more slowly. In general rough surface grow faster than smooth one. So final growth form consists entirely of slow growing faces. The presence of screw dislocation in the crystal provides step which spiral under flux of adatoms. This provides a mechanism of continuous growth of modest supersaturation. During crystal growth by spiral movement growth velocity depends quardetically with supersaturation. And crystal growth on terrace growth velocity depends exponentially with supersaturation. Dislocation are dominant at low supersaturation.Growth form the liquid and from the solution has been similarly treated emphasizing the internal energy change on melting, alpha factor is proportional to internal energy change where the value of alpha is less than 2 for melt growth of elemental solids corresponds to rough liquid –solid interfaces. Growth form the vapour via smooth interface are characterized by large alpha value because the sublimation energy and growth temperature is much lower than the melting temperature. To represent growth kinetics different notation have. It is convenient to use z-axis as surface normal leaving x and y for direction in surface plane. No need for lattice spacing c(z) to be constant.

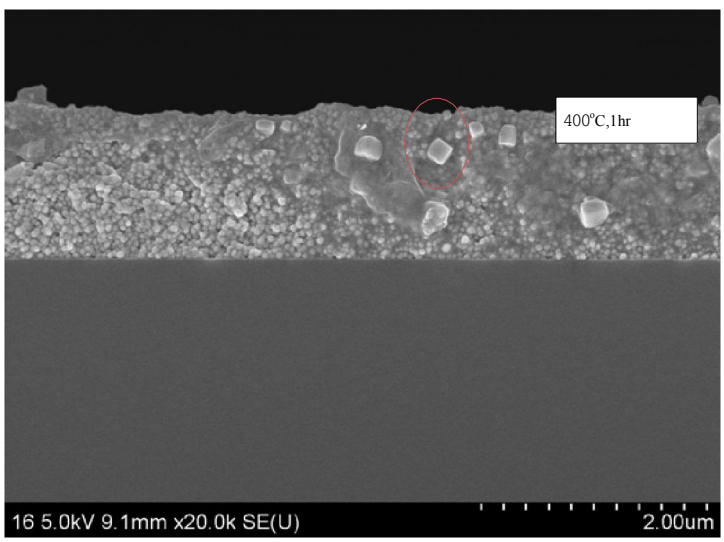

Fig. 33. Faceted growth behavior of Ag sintered at 400°C for 1 hr in N2

Grain boundary faceting is shown in Fig. 34. Fig. 34. shows that twining is parallel to faceted grain boundary so this grain boundary will be Σ3 grain boundary.. Here also different crystal growth notaion is important. m is used to designate layer number. Starting m=1 from surface. c(m) reflects the bonding of perticular crystal and the specific crystal face. It is not necessary that lateral periodicity in (x,y) is the same as bulk periodicity (a,b). On the other hand because the surface layer are close contact with the bulk there is a strong tendency for the periodicity to be, if not the same ,a simple multiple, sub multiple or rational fraction of a and b , a commensurate structure. Lattice constant are defined with respect to perticular {h k l} surface. Notion to define surface originates (2X2) matrix M ,where M relating to surface parameter. Many structure of (001) have a centered rectangular structure. We can reduce the structure to simple square by rotating the axis through 45 degree. (1X1): This is a bulk termination. This does not mean that the surface is similar to bulk in all respect, merelly that the average lateral periodicity is the same as bulk. Silver (111) shows bulk termination structure. Bcc metal such as Mo(001) also shows (1X1) structure at high temperature but have phase transition to (2X1) and related incomensurate structures at low temperature. Lower symmetries are more common at low temperature than at high temperature. The interaction between atmos is strongly anharmonic, leading perhaves to double well interaction potential. At high temperature the vibration of atom span both the wells, but at low temperature atom choose one or the other. The c spacing of metal (1X1) surface have been extensively studied are found mostly to relax inwords by several percentage. This is the general feature of metalic binding,where what counts primarily is the electron density around the atom rather than the directionality of bonds. The atom like to surround themself with perticular electron density because some of this is removed in forming surface and surface atom snuggle up closer to compensate. For silver sigma 3 grain boundary faceting is observed[47] on (011) faceted surface. The grain boundary facet plane are expected to be singular corresponding to cups in polar plot of the boundary energy against inclination angle. If this boundary step move by boundary step mechanism, then abnormal grain growth may occur. The magnitude of the burgers vector of the secondary grain boundary decreases as the CSL density decreases. Since there is only a limited number of high density CSL ,there is only a limited number of cases where a grain boundary have a relatively large b. The secondary grain boundary grid spacing decreases as the deviation from CSL orientation increases. At present there is no firm basis on deciding of magnitude of minimum b which is physically realistic .

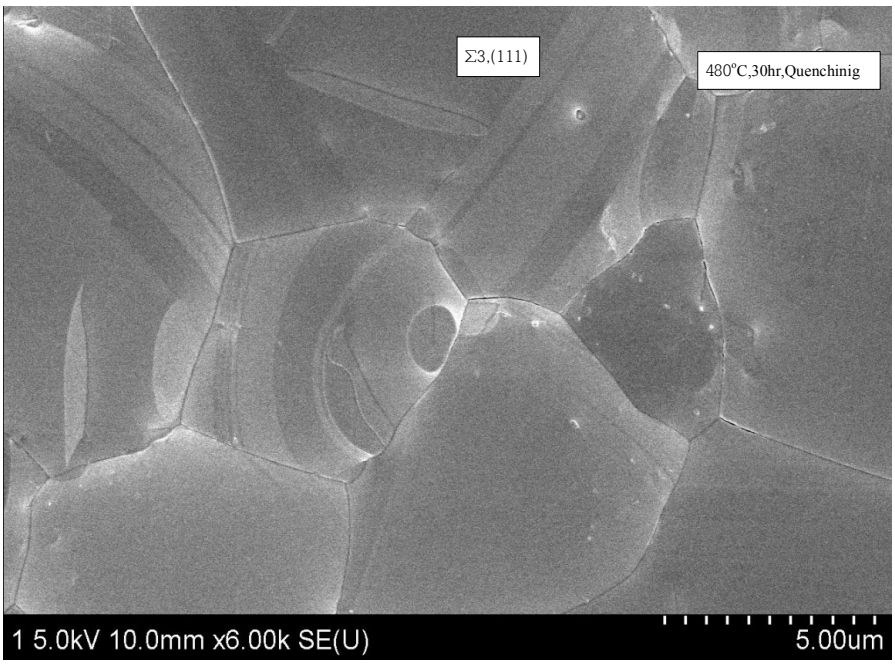

Fig. 34. Grain boundary faceting of Ag sintered at 480°C for 30 hr in N2

F. Roughening transition temperature for silver

Roughening transition temperature can simplely be defined as the temperature at which crystal transform from faceted to rough interface. Singular surface generally form faceted surface and singular surface is responsible for abnormal grain growth through a process of 2D nucleation. 2D nucleation is a slow growth process in which flat one atomic sheet joined on singular surface. (115),(110),(111) are the low index planes of silver. The planes which have lowest surface tension that will be removed later if we increase temperature. As it is expected for silver to change shape gradually from faceted to sphere shape.

According to

Sub section F(1) $T_{(R)} > 500^{o}C$. (N_2 atm.)
Sub section F(2) $T_{(R)} = 475^{o}C$ (O_2 atm.)
Sub section F(3)$T_{(R)} > 475^{o}C$ (N_2 atm.)
Sub section F(4) $T_{(R)} > 475^{o}C$ (O_2 atm)
Sub section F(5) $T_{(R)}$ = Between 500^{o} to $600^{o}C$. (N_2 atm.)

So, we can conclude roughly that in oxygen atmosphere roughening transition temperature is between $400^{o}C$ and $500^{o}C$ but for Nitrogen atmosphere it is between $500^{o}C$ and $600^{o}C$. So, We can consider roughening transition temperature in nitrogen environment is $500^{o}C$ and in oxygen furnace atmosphere is $475^{o}C$.

1. Quencing behavior (nitrogen atmosphere)

All specimen were prepared here using silver nanopaste S2. We have quenched Specimens using water in different atmosphere. However, in Fig. 35 SEM images of quenched specimen that are soaked at $350^{o}C$, $400^{o}C$, $450^{o}C$ and $500^{o}C$ are shown. Quenching is a suitable process to see high temperature microstructure at room temperature. However, if the furnace cooling rate is faster than critical cooling rate then water quenched and furnace cooled structure will be same. Because then both cooling rate will be faster than critical cooling rate. In this case we have used nitrogen atmosphere as furnace

environment.

2. Quencing behavior (oxygen atmosphere)

All Specimens were prepared here using silver paste S2. We have use 100 sccm oxygen flow during soaking then quenched the sample after one hour soaking directly in to water. (Fig. 36). Here we have seen that particle colesence is difficult because oxygen decrease the surface tension. So particle want to separate compare to nitrogen environment that also result smaller size particle comparablely. So after sintering 475^{o}C we observed fine scale texturing on every particle.

3 Furnace cooling behavior (nitrogen atmosphere)

All samples were prepared here using silver paste S2. Furnace cooling process is slower cooling process compare to quenching process. Fig. 37. shows the SEM images of furnace cooled specimens for different temperature under nitrogen atmosphere.

4. Furnace cooling behavior (oxygen atmosphere)

All Specimens were prepared here using silver paste S2. Fig. 38 shows furnace cooled SEM Specimens for different sintering temperature under oxygen atmosphere.

5. Furnace cooling behavior in nitrogen atmosphere

All Specimen were prepared here using silver paste S1. Fig. 39 shows furnace cooled silver Specimens under nitrogen atmosphere to determine roughening temperature by observing external shape of silver nano particle.

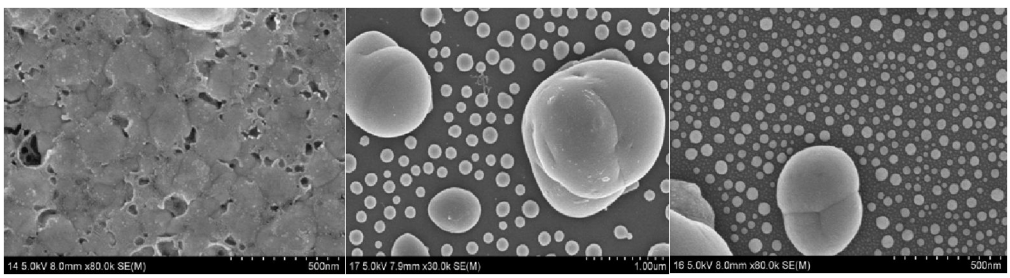

350°C 400°C 450°C

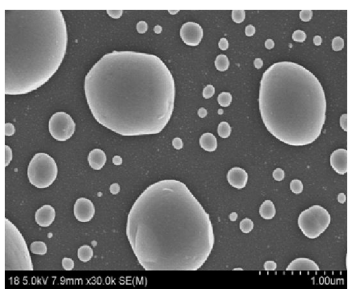

500°C

Fig. 35. Quencing behavior of silver nanoparticle in nitrogen atmosphere.

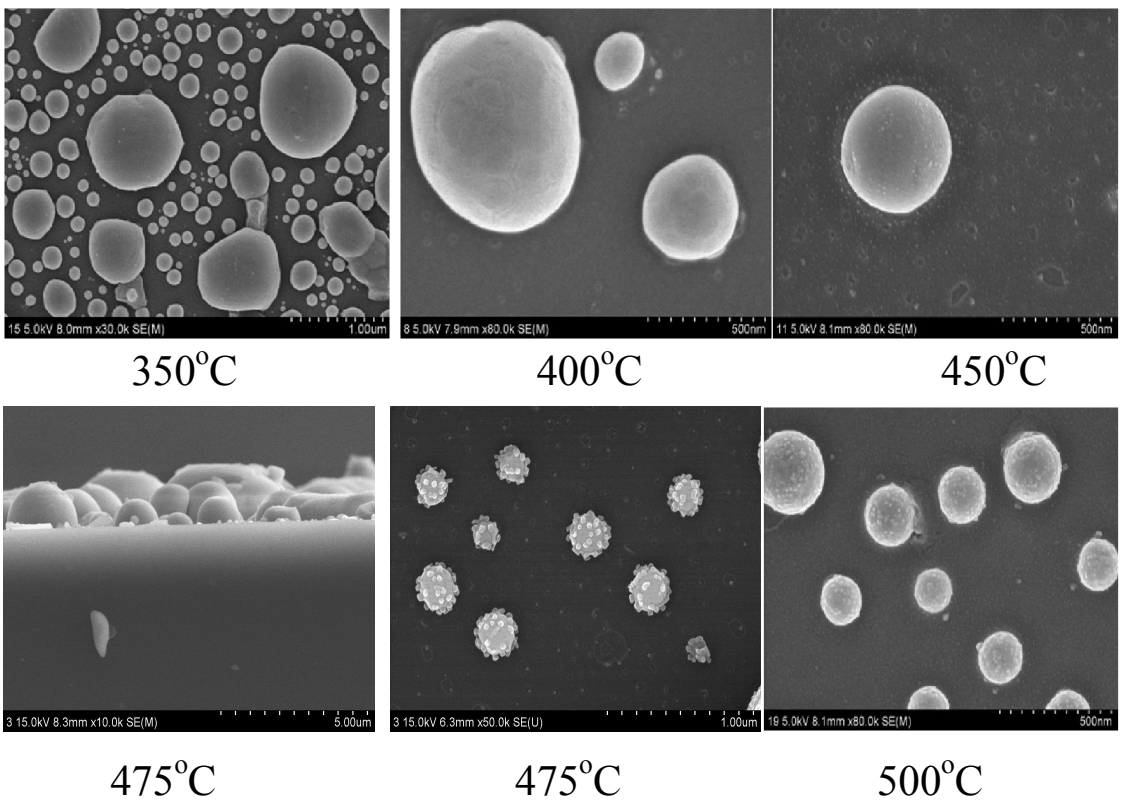

Fig. 36. Quencing behavior of silver naoparticle in oxygen environment.

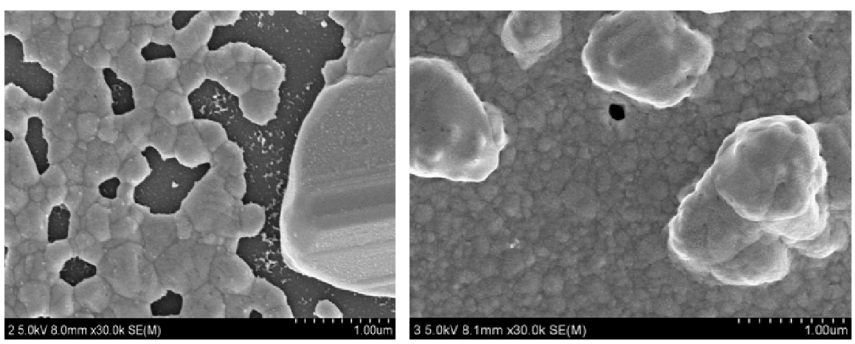

Fig. 37. Furnace cooling behavior of silver nanoparticle in nitrogen atmosphere.

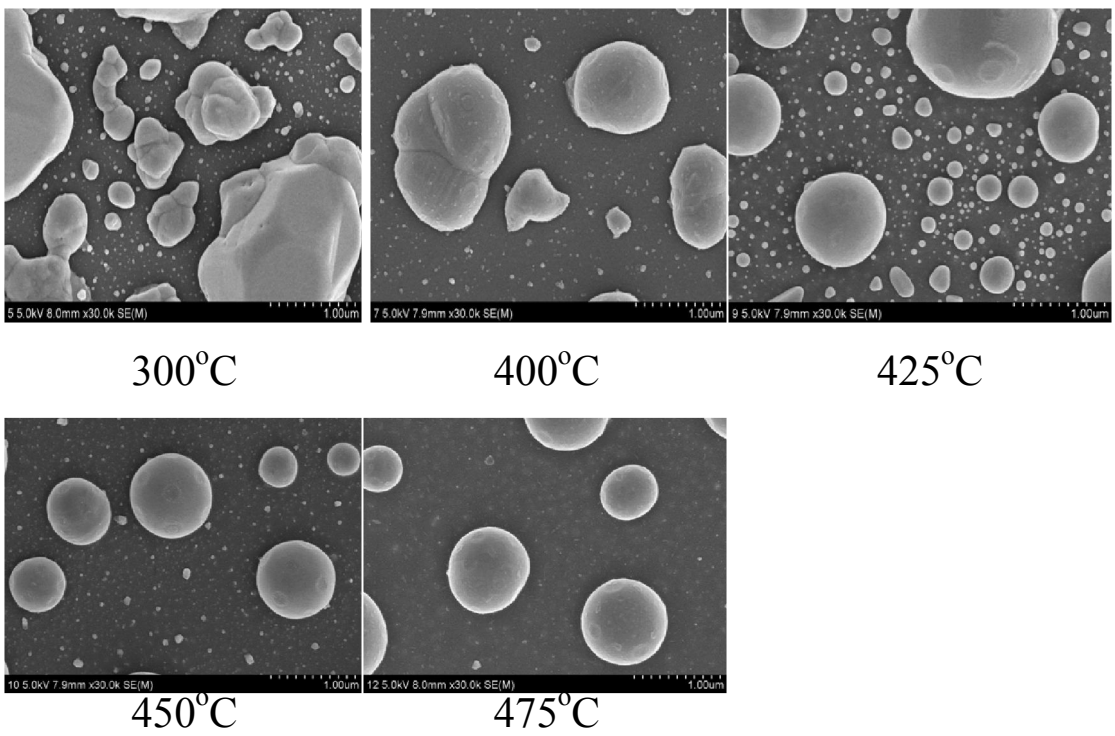

Fig. 38. Furnace cooling behavior of silver nanoparticle in oxygen atmosphere.

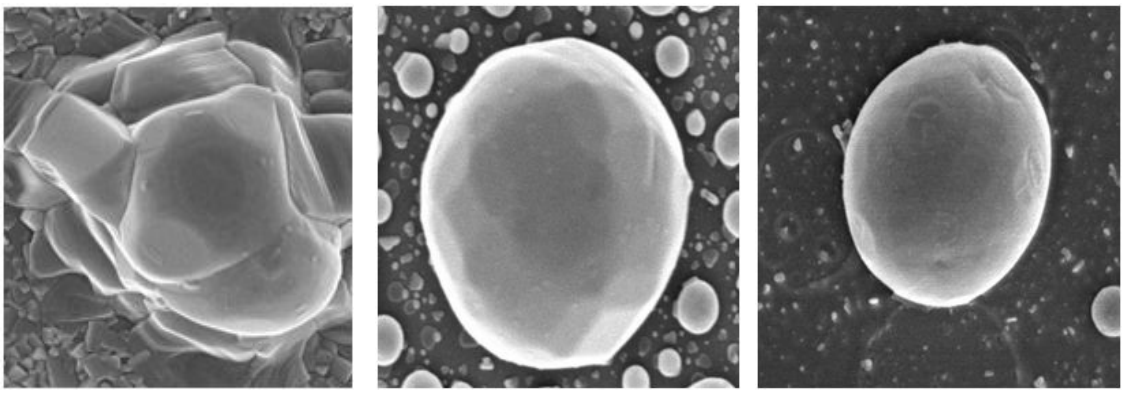

(a) 450°C (b) 500°C (c) 600°C

Fig. 39. Shape change of a large silver grain in nitrogen atmosphere.

V. Conclusion

The use of silver in printed circuit broad as well as in OLED, Plasma display is increasing day by day due to its suitability. It can be used as anode and cathode for organic solar cell. Because very thin film of silver is transparent. The increase of use of silver increases the necessity to do more research on it. Silver nanoparticle research can open a new door because nanoparticle shows different property compare to polycrystalline silver. In this experiment, we have seen that the roughening transition temperature of silver nanoparticle is lowerer compare to polycrystalline silver. Again we have produced different shape particle by controling the abnormal grain growth. We have seen that low temperature grain growth mechanism is completely different from high temperature grain growth mechanism which is occurred above roughening transition temperature. We have also seen that faceting not only increase conductivity but also change surface morphology from plane to textured surface. Use of oxygen atmosphere as sintering atmosphere compare to nitrogen atmosphere facilities to form normal grain growth by decreasing roughening transition temperature and decrease the particle size[31]. The reason is, silver oxide formation on surface. It lowers the surface tension of grain then particle can easily separated from each other quickly comparablely. So the effect of faceted grain formation either by using nitrogen or oxygen not only can change property but also can change the shape and morphology of thin film.

References and Notes

1. I. Sunagawa,"Growth and Morphology of Crystals", Review Forma 14, 358 (1999).
2. Y. Natsume, K. Ohsasa, H. Esaka and T. Narita, "Analysis of Growth Behavior of a celluler and Dendritic Interface under a constrained Growth using a Phase field model" Materials Transactions 44, 5 (2003).
3. I.K. Bonev and C.M. Rice, "Single Crystal Galena Pillars as Highly Anisometric Dissolution Forms", Mineralogical Magazine 61, 406 (1997).
4. X.Y. Liu and P. Bennema, " Observation of Roughening transition and influence on Morphology of Crystals", J.Crys. Growth 139, 1-2 (1994).

5. M. Elwenspoek and J.P. Vander Eerden, "KineticRoughening and Step free energy in the solid on solid model and on naphthalene crystals", J.Phys.A: Math. Gen. 20 (1987).
6. K.S. Liang, E.B. Sirota, K.L. D'Amico , G.J. Hughes and S.K. Sinha, "Roughening Transition of a stepped Cu(113) Surface: A Synchrotron X-ray-Scattering Study", Phys. Rev. Lett. 59, 21 (1987).
7. J. Arsic, I.C. Reynhout, W.J.P. van Enckevort and E. Vlieg, "Equilibrium Morphologies and Thermal roughening of Cesium Halides", J. Crys. Growth 245 (2002).
8. Y.K. Cho, D.Y. Yoon and B.K. Kim, "Surface Roughening transition and coarsening of NbC grains in liquid cobalt- rich matrix", J. Ame. Ceram. Soc. 87, 3 (2004).
9. R. Warren,"Microstructural Development During Liquid Phase Sintering of two phase alloys, with Special Refer Reference to NbC/Co System", J. Mat. Sci. 3, 5 (1968).
10. S.J. Zheng, K. Du, X.L. Ma, "Abnormal Grain Growth of BaTiO3 by 2D nucleation and lateral growth", J. Euro. Ceram. Soc. 28 (2008).
11. S.B. Lee, D.Y. Yoon, N.M. Hwang and M.F. Henry, Grain boundary faceting and Abnormal grain growth in Nickel", Meta. Mat. Trans. A 31, 3 (2000).
12. G.D. Hibbard, J.L. McCrea, G. Palumbo, K.T. Aust and U. Erb,"An initial analysis of mechanisms leading to late stage abnormal grain growth in nanocrystaline Ni", Scripta Materialia 47 (2002).
13. D.M. Kirch, B. Zhao, D.A. Molodov and Gottstein,"Faceting and Migration of low angle <100> Tilt Grain Boundaries in pure Aluminum",Mat. Sci. Forum 558-559, 903 (2007).
14. B. Grossmann, H. Gu and M. Grant,"Kinetic Physical Review A 43,4 (1991).
15. S.B. Lee, "Corelation between Grain boundary faceting and defaceting transition and change of grain boundary properties with temperature", Mat. Lett. 57 (2003).
16. D. Bouchet and E. J. Thibault,"A HREM Study of a nearly perfect S = 11 tilt bicrystal in nickel", Microsc. Microanal. Microstruct. 3, 1 (1992).
17. T.P. Pearl, S. B. Darling and S.J. Sibener, "Step-modified phase diagram of chemi-absorbed Oxygen on Nickel" Surface Science 491 (2001).
18. M. Okada, L. Vattuone, M. Rocca and Y. Teraoka," Effect of Step geometry in Copper Oxidation by Hyperthermal O2 molecular beam: Cu(511) vs Cu(410)", J. Chem. Phys. 136, 9 (2012).
19. W.E. Boggs, R.H. Kachik and G.E. Pellissier,"The effect of Crystallographic Orientation and Oxygen Pressure on the oxydation of iron",J. Electro. Soc. 114, 1

(1967).
20. A.A. Wheeler,"Phase field Theory of Edges in an aniso- tropic crystal", Proc. R. Soc. A 462, 2075 (2006).
21. S. Torabi, S. Wise, J. Lowengrub, A. Ratz and A.Voigt,"A new method for simulating Strongly Anisotropic Chan-Hilliard Equations", Mat. Sci. & Tech. 3 (2007).
22. N.M. Hwang, Y.J. Park, D.Y. Kim and D.Y. Yoon,Activated Sintering of nickel-doped tungsten: Approch by grain boundary structural transition", 42, 5 (2000).
23. G.D. Hibbard, V. Radmilovic, K.T. Aust and U. Erb," Grain Boundary Migration during abnormal grain growth in nanocrystalline Ni", 494, 1-2 (2008).
24. G.H. Gilmer,"Computer Simulation of Crystal growth", J. Crys. Growth 42 (1977).
25. K. Maiwa, M. Plomp, W.J.P. van Enckevort and P.Bennema , "AFM observation of barium nitrate {111} and {100} faces:: spiral growth and two-dimensional nucle-ation growth", J. Crys. Growth 186, 1-2 (1998).
26. J.F. Banfield, S.A. Welch, H. Zhang, T.T. Ebert and R.L. Penn,"Aggregation-based Crystal Growth and Microstructure Development in Natural Iron Oxyhydroxide Biomineralization Products", Science 289, 5480 (2000).
27. G.H. Gilmer,"Transients in the rate of crystal growth",J. Crys. Growth 49, 3 (1980).
28. D. Peng, S. Osher, B. Merriman and H.K. Zhao, ″ The Geometry of Wulff Crystal Shapes and Its Relations with Riemann Problems ‶ ,*Citseer* 18-7 (1998).
29. D.H. Warrington, ″ The Coinsidence Site Lattice (CSL) Grain Boundary (DSC) Dislocations For The Hexagonal Lattice ‶, *J. De Physique* 36, 10 (1975).
30. H.A. Mendez-Pinzon, D.R. Pardo-Pardo, J.P. Cuellar-Alvarodo, J.C. Salcedo-Reyes, R. Vera and B.A. Paez- Sierra, ″ Analysis of current-voltage characteristics of polymer-based organic light-emitting diodes (OLEDs) deposited by spin coating ‶, *Javeriana* 15, 1 (2010).
31. M. Turker,“Effect of oxygen content on the sintering behavior of silver nanopowder produced by Innert Gas Condensation”, *Turkish J. Eng. Env. Sci.* 26(2002).
32. S.H. Avner,“Introduction to Physical Metallurgy”,Second Edition,McGraw-Hill,Inc. p249-255.
33. M.J. Kirchhof, H. Forster, H.J. Schmid and W. Peukert,“Sintering Kinetics and Mechanism of vitreous nanoparticles”,*J. Aero. Sci.* 45(2012).
34. Y. Akada, H. Tatsumi, T. Yamaguchi, A. Hirose, T. Morita and E. Ide,“Interfacial Bonding Mechanism using Silver Metallo-Organic Nanoparticles to Bulk Metals and Observation of Sintering Behavior”, *The Japan Institute of metals* 49(2008).

35. Steve Lien-Chung Hsu, Rong-Tarng Wu,"Preparation of Silver Nanoparticle With Different Particle sizes for Low-TemperatureSintering" International Conference on Nanotechnology and Biosensors IPCBEE v.2 IACSIT Press Singapore(2011)
36. P.E. Lewis, P.M. Lee,"Band Structure and Electronic Properties of Silver",*Physical review* , vol 175, number 3, (1968).
37. L. Hodges, H. Esrenreich and L.D. Lang,"Interpolation Scheme of Band Structure of Nobel and Transition Metal: Feromagnatism and Neutron Diffrection in Ni." *Physical rev*,v152,n3.(1966)
38. A.D. Rollett,"Abnormal grain growth and texture development"*Materials Science forum*,v495-497pp1171-1176 (2010).
39. J.C Dutra, F. Siciliano Jr and A.F. Padilha,"Interaction Between Second phase Particle Dissolution and Abnormal grain growth in an Austanitic stainless Steel"Mat.res.v5,n3,(2002).
40. J. Perelaer, C.E. Hendriks, A.W.M. de Laat and U.S. Schubert,"One step inject printing of conductive silver tracks on polymer substrate" Nanotechnology vol20, 1653031-1653035 (2009).
41. J.M. Kohler, L. Abahmane, J.wagner, J.Albert, G.Mayer," Preparation of metal nanoparticle with varied composition for catalitic application in microreactor".*Chemical engineering science*, v63,I2.(2008).
42. Jolke Perelaer, Antonius W.M. de Laat, Chris E. Hendriks and Ulrich S. Schubert," Inkjet Printed Silver Tracks:low temperature curing and thermal stability investigation" *Journal of Materials Chemistry* (2008).
43. T.P. Schulze, R.V. Kohn," A geometric model for coarsening during spiral mode growth of thin film" *Physica D* 132 520-542(1999).
44. A.Resinger, O. Ricken, P. Kuhn, A. Raetz, A. Voigt, J. Krug, T. Michely,"Spiral growth and step edge barrier"*Phys Rev. Lett*,100(2008)
45. Jeri Cejka,Avelino Corma, Stacey Zones,"Zeolites and Catalysis" V1, Chapter1, pp1-52, Willy-VCH.(2010)
46. h.P. Bongel,"3D equilibrium crystal shape in the new light of STM and AFM,"*Physics Report*,V385, I1-2(2003).
47. A.I. Barg, E. Rabkin, W. Gust,"Faceting transformation and energy of sigma 3 grain boundary in silver" *Acta Metallurgica et Materialia*,v43,I11(1995).

Acknowledge

I am very much grateful to Prof. Yong-Taeg Oh for his support.